

# **Model Identification of Leukemia Transcription Factor Networks**

Katharine V. Rogers, Adithya Sagar, Holly A. Jensen, and Jeffrey D. Varner\*

School of Chemical and Biomolecular Engineering  
Cornell University, Ithaca NY 14853

**Running Title:**

**To be submitted:**

\*Corresponding author current address:

Jeffrey D. Varner,  
Professor, School of Chemical Engineering,  
1158 Forney Hall, Purdue University, West Lafayette IN, 46907  
Email: jdvarner@purdue.edu  
Phone: (765) 496 - 0544

## **Abstract**

**Keywords:** leukemia, cancer, mathematical modeling

## **1 Introduction**

2 It was suggested by Bailey, more than a decade ago, that qualitative and quantitative  
3 knowledge of complex biological systems could be achieved in the absence of complete  
4 structural and parameter knowledge [4]. Although this is true, the incomplete knowledge  
5 of biological phenomenon often limits the impact of computational models. Unknown or  
6 even disputed network structures can lead to incomplete fitting of computation models,  
7 requiring additional experiments and updating of the model. Since ODE kinetic models  
8 typically require extensive prior knowledge of network structure, rate constants and ini-  
9 tial conditions [55], often a single “correct” network structure is assumed. Villaverde *et*  
10 *al.* discussed three main strategies in the reverse engineering of dynamic models: (1)  
11 full network inference, (2) network selections, and (3) kinetic parameter estimations [93].  
12 Strategy 1, where the kinetic model structure and kinetic parameters are unknown, is  
13 typically solved by identifying the model interaction network without dynamics and then  
14 identifying the kinetic parameters. In this study, we will consider strategy 2; we have an  
15 initial model network structure that will be perturbed to find modifications to fit the experi-  
16 mental data for six different leukemia cell lines.

17 Leukemia is the 6th leading cause of cancer death in both males and females in the  
18 United States [82]. Approximately 72% of cancer related leukemia deaths were caused  
19 by four main types of leukemia; acute lymphocytic leukemia (ALL), chronic lymphocytic  
20 leukemia (CLL), acute myeloid leukemia (AML), and chronic myeloid leukemia (CML). ALL  
21 and CLL are characterized by accumulation of lymphocytes in the bone marrow, with ALL  
22 progressing at a faster rate (i.e. acute vs. chronic). ALL occurs in both children and adults  
23 and has a 90% five year survival rate in children [46], while CLL is rare in children and  
24 has a 66% five year survival rate (2001-2009) [69]. The 10 year survival rate for CML has  
25 improved to 80-90% due to the use of targeted treatments for BCR-ABL and adenosine  
26 triphosphate (ATP) [47]. AML is characterized by the accumulation of abnormally differen-

27 tiated cells of the hematopoietic system in the bone marrow and blood, with a survival rate  
28 of 35 to 40% in adults under the age of 60 (5 to 15% in patients older than 60) [30]. AML is  
29 a group of extremely heterogeneous diseases, with over 200 known chromosome translo-  
30 cations and mutations in patient leukemic cells [41]. The use of differentiation induction  
31 therapy agents like all-*trans* retinoic acid (RA) and 1,25-dihydroxyvitamin D3 (D3) have  
32 been explored in many cancer cell types, including myeloid leukemias, and lung, liver,  
33 prostate, and breast cancer (RA treatment) [16, 88] and in prostate, breast, colorectal,  
34 leukemia, and brain (D3 treatment) [20]. Acute promyelocytic leukemia (APL), a subtype  
35 of AML, was once one of the most fatal forms of acute leukemia until the introduction of  
36 RA increased remission rates of patients to between 80 and 90 % [21]. Failure of RA  
37 treatment can occur initially in patients with RA resistant variants (PLZF-RARA-positive  
38 APL), and relapse occurs in 5-20% of cases due to the emergence of RA resistance. To  
39 understand the response of multiple leukemia cell lines to RA and D3 treatments, we de-  
40 veloped a network structure of well known transcription factors governing myelomonocytic  
41 lineage selection (granulocytic or monocytic).

42 In this study we considered data from RA, D3, and RA plus D3 treatments on six hu-  
43 man myeloid leukemia cell lines; (1) K562 (FAB M1), (2) HL60 (FAB M2), (3) NB4 (FAB  
44 M3), (4) U937 (FAB 5), (5) HL60 R38+ and (6) HL60 R38- (5 and 6 are described previ-  
45 ously [49]). K562, a CML cell line with a Bcr-Abl fusion protein [62], was used as a control  
46 because the cells are not responsive to both RA [77] and D3 treatment [68]. HL60 cells,  
47 an AML cell line, are lineage-bipotent myelobasts [25, 36] that can differentiate to either  
48 granulocytic lineage (using RA) or monocytic lineage (using D3). The two RA-resistant  
49 HL60 cell lines, R38+ and R38-, were described previously [48, 49]. NB4, an APL cell  
50 line, are highly RA-responsive, but require combination treatments for monocytic differen-  
51 tiation (i.e. low response to D3) [11, 89]. U937, histiocytic lymphoma cell line, are highly  
52 responsive to D3 induced monocytic differentiation, but have ambiguous differentiation

53 effects due to RA (either monocytic or granulocytic) [26, 70, 71]. The model network con-  
54 tained two inputs (RA and D3) and 18 main species. We included two receptors, reinoic  
55 acid receptor alpha ( $RAR\alpha$ ) and vitamin D receptor (VDR), but excluded their heterodimer  
56 receptor pair, retinoid receptor (RXR), for simplicity (assumption RXR is readily available).  
57 Also, included in the model were transcription factors important in myelomonocytic lineage  
58 selection (listed in Table 1). Finally upstream markers for differentiation were included, in-  
59 cluding CD38, CD11b, CD14, G1/G0 cell cycle arrest and inducible oxidative metabolism.  
60 CD38 and CD11b are myelomonocytic markers and CD14 is a monocytic specific marker.

61 In this study we first determined that a network structure of a small three node protein  
62 model could be identified with sufficient experimental data. A model structure search in  
63 combination with particle swarm optimization to determine parameter values narrowed  
64 down total possible model structures from 19683 to twenty. After additional experimental  
65 data was implemented, we were able to find the synthetic model structure with no *a priori*  
66 knowledge. Next we investigated possible network structures for transcription factor and  
67 upstream markers in six leukemia cell lines treated with RA and D3 (data from [50]). The  
68 upstream markers CD38 and CD11b (myelomonocytic markers) and CD14 (monocytic  
69 specific marker) were included in the model. Also, included in the model were transcription  
70 factors important in myelomonocytic lineage selection. Starting from an initial best model  
71 structure curated from literature sources, we were able to improve the model fits for six  
72 leukemia cell lines versus experimental data.

## 73 **Results**

74 **0.1 Three Node Example Network** To determine if we could distinguish between pos-  
75 sible model structures, we began by first modeling a simple three protein node network.  
76 The model we designated as the true model is shown in Figure 1A and the results for the  
77 synthetic data generated are given in Figure S1. All proteins in the model could act as ei-

ther transcription factors or transcription repressors. The two examples of transcriptional regulation, activation and repression, are given in Figure 1D. Assuming no prior knowledge, other than number of nodes and inducer location, we were able to narrow down possible network structures with just one experiment and ultimately determine the true network structure with a small set of additional experiments (Table T3). For an  $n$  node protein network with three possible interactions between nodes (activation, inhibition, or no interaction) and allowing for self regulation (i.e.  $P_1$  can be a transcription factor for itself), we had a total of  $3^{n^2}$  possible structures, where  $n$  is the number of protein nodes. The simple  $n = 3$  case had a total of 19683 possible model structures, which we exhaustively searched and determined a best fit parameter set for each model using particle swarm optimization. For particle swarm optimization we designated a ten particle system and 30 operations, for 300 total iterations. The initial ten particles were each a set of parameters containing 35 randomized parameters (20 control parameters and 15 kinetic parameters). Using the data from five species (one saved for validation) in experiment 1 (Table T3), we narrowed our results to the 20 best model structures (top 0.1%). For these 20 best models, we ran a second particle swarm optimization with 300 total iterations to determine if a better solution could be found. In this case we started with ten particles randomized from the best parameter set from each model obtained from the first trial. As shown in Figure 2, the true model was not selected as the best fit and we did not find the “true” parameter set. The top model was similar to the true model with two additional interactions and two opposite sign interactions (i.e. activation instead of inhibition) (Fig. 1B). Therefore, by using data from just one experiment we were able to obtain a subset of 20 possible model structures.

From the possible 20 model structures we wanted to determine if we could narrow down the possibilities to one structure with the use of additional experimental data. All top 20 models show qualitatively the correct response (Fig. 2) and therefore, the simulation

error could be caused either by a model structure issue or a parameter set estimation issue (did we find the correct parameters?). The top 20 models have many features in common (Fig. 3): (1) All 20 models designated  $P_1$  as a transcription factor activator for species two, (2) 19 models showed  $P_2$  inhibits itself, (3) 20 models showed  $P_2$  as a transcriptional regulator (activator or repressor) for species three, with four having the opposite interaction (i.e. repression instead of activation), and (4) 18 models showed  $P_3$  regulated itself, but 12 of these cases are opposite (activation instead of repression). Many of the structures also had added interactions: (1) ten models added regulation from  $P_3$  to species two, (2) eight models added self-regulation of  $P_1$  (all activation), and (3) eight models added regulation of species three by  $P_1$ . After studying the possible structures we performed two additional experiments to obtain synthetic data (Table T3). In experiment two an inducer was added at t=100 A.U. and the binding domain of  $P_2$  was inhibited (i.e.  $P_2$  could not act as a transcription factor). Finally, in experiment three an inducer was added every 24 A.U. starting at t = 100 A.U., to represent step inputs on the system. Again we ran a particle swarm optimization method to find a new best fit parameter set for the top 20 models, this time using a total of three experiments and five species per experiment to calculate experimental error (Table T1). With the additional two experiments we were able to exclude the previous top model (Fig. 1B). In figure 4C and 4F, we see that the previous top model (in blue) does not qualitatively fit mRNA or protein data for species three. The true model (red) is the second best fitting model after optimization with three experiments, while the new top fitting model is in green. In experiment two,  $mRNA_3$  decreased due to the inhibition of  $P_2$  activity ( $P_2$  is a transcription factor activator for  $mRNA_3$  in the true model). The previous top model (3147) was not able to obtain this result due to the incorrect interaction between  $P_2$  and species three (inhibition instead of activation). The new top model (Fig. 1C) had one additional interaction that occurred between  $P_3$  and species two. After finding that the control parameter value,  $\kappa_{3,2}$ , was 9.9e-7 (essentially

130 zero), for this interaction we were able to ignore the additional interaction (in equation 14,  
131 if  $\kappa_{3,2} = 0$  then  $f_{3,2} = 0$ ). Therefore, with using only three experiments and 15 objective  
132 functions we were able to obtain the correct model structure after exhaustively searching  
133 all 19683 possible structures. From the small three node network we determined that  
134 the correct model structure could be identified with sufficient experimental data after an  
135 exhaustive network search.

136 **0.2 Leukemia Transcription Factor Network** Next we investigated possible network  
137 structures for transcription factor and upstream markers in six leukemia cell lines treated  
138 with RA and D3 (data from [50]). The six cell lines, K562, HL60, NB4, U937, HL60 R38+  
139 and HL60 R38-, had diverse reactions to the stimuli and thus, we assumed that network  
140 structures could differ between cell lines. The leukemia transcription factor network with  
141 two inducers (RA and D3), contained 42 differential equations (RXR was included but set  
142 to zero in this case), 652 control parameters, and 90 kinetic parameters. In this case, with  
143  $n = 18$  protein nodes, if no prior knowledge was assumed, other than number of nodes  
144 and inducer location, we would have a total of  $3^{18^2}$  possible model structures. To nar-  
145 row down our search space we first assumed proteins which do not act as transcription  
146 factors always have no interaction from the protein to another species: CD38, CD11b,  
147 CD14 and p47. Also, we designated the protein Gfi-1 as always acting as a repressor if  
148 the interaction existed. Next we created an initial guess transcription factor network by  
149 searching the literature, which is shown in Figure 5 (interactions and references shown in  
150 Table 1). We began by calculating a top parameter set for each cell line using this initial  
151 network structure. A top parameter set was calculated using particle swarm optimization  
152 with 35 particles and 90 iterations per particle, for a total of 3150 iterations. Simulation  
153 data for each cell line was compared to 39 objective functions found in Table T4. After  
154 finding the parameter set with the lowest error for each model based on this initial struc-  
155 ture, we then perturbed the model by randomly changing one to three edges in the model

156 from our initial best guess to either no interaction (0), negative interaction (-1), or positive  
157 interaction (1). Again we used particle swarm optimization to find a new best parameter  
158 set for the updated model. If the error was less than the previous model we accepted the  
159 new model, and in the next iteration we would perturb this new model structure. Through  
160 this method, we looked at approximately 300 model structures for each cell line and were  
161 able to improve model fits compared to the initial model structure.

162 Through model and parameter optimization we discovered improved network struc-  
163 tures for the six cell lines: K562, HL60, NB4, U937, HL60 R38+ and HL60 R38-. The new  
164 network structures showed improved fits against a subset of the experimental data. For  
165 example the new model structure of the HL60 R38- cell line was able to accurately predict  
166 the increase in VDR concentration due to a D3 stimulus and RA+D3 stimulus which was  
167 missed in the original structure (Figure 6). The new model structure for the HL60 cell line  
168 was able to predict the CD38 expression shift due to RA and RA + D3 stimulus, but still  
169 missed the D3 stimulus experiment (Figure 7). In the NB4 case of CD11b concentration  
170 we again missed the D3 stimulus experiment, but were able to improve the results of the  
171 RA and RA + D3 stimulus experiments (Figure 8). Change in PU.1 concentration due to  
172 RA, D3, and RA + D3 treatments was accurately modeled with the new K562 model struc-  
173 ture (Figure 9). Training experiments involving AhR in U937 cells and C/EBP $\alpha$  in HL60  
174 R38+ cells are also shown (Figure S2 and S3). To improve the model fits many pertur-  
175 bations (adding, deleting, or switching edges) were made to the initial network structure  
176 for each cell line. For the K562 cell line, unresponsive to RA and D3, 100 changes were  
177 made to our initial best network structure (Table T5). The model structure for the NB4 cell  
178 line, which is highly responsive to RA, contained 90 changes (Table T6). For HL60 cells,  
179 91 edges were changed in the model structure (Table T7). The two RA resistant HL60,  
180 R38- and R38+, models had 76 and 74 changes, respectively (Table T9 and Table T8).  
181 Finally, the U937 model had 41 network changes in the best model solution (Table T10).

182 Taken together, through a combination of network perturbations we were able to better  
183 predict a subset of experiments in six leukemia cell lines: K562, HL60, NB4, U937, HL60  
184 R38+ and HL60 R38-. We also developed new model structures specific to each cell line  
185 from our initial shared model structure guess.

186 **Discussion**

187 In this study, we developed a method for determining protein node network structures  
188 from experimental data with incomplete biological knowledge. The models described  
189 transcriptional regulation due to the input of inducers. First we were able to determine  
190 a toy three node protein network structure by searching through all possible structures  
191 and using particle swarm optimization to optimize parameters. The network structure was  
192 narrowed down to a subset of 20 models using data from one experiment and eventually  
193 found using two additional experiments. In total, 15 objective experiments were used for  
194 training and three experiments were saved for prediction. Of the top 20 network structures  
195 found many of the edges were conserved including: (1) All 20 models designated  $P_1$  as  
196 a transcription factor activator for species two, (2) 19 models showed  $P_2$  inhibits itself, (3)  
197 20 models showed  $P_2$  as a transcriptional regulator (activator or repressor) for species  
198 three, with four having the opposite interaction (i.e. repression instead of activation), and  
199 (4) 18 models showed  $P_3$  regulated itself, but 12 of these cases are opposite (activation  
200 instead of repression). In many cases additional interactions were added. By adding  
201 data from two additional experiments to the training, we were able to narrow down the  
202 results further with the true model as the second best result. After determining the two  
203 models differed in only one additional interaction, which was essentially zero due to the  
204 kinetic parameter, we were able to exclude this interaction and therefore found the true  
205 model. One note, we were not able to find the true parameter set that was used to  
206 obtain the synthetic data with the number of iterations performed. Additional parameter

207 estimation and the use of an ensemble of parameter sets may be necessary to find a more  
208 optimal parameter solution. From this we determined that the correct network structure of  
209 a small transcriptional regulation network could be found with enough experimental data  
210 and model iterations.

211 Next we applied this method to determine transcription factor network structures for  
212 six leukemia cell lines: K562, HL60, NB4, U937, HL60 R38+ and HL60 R38-. All six cell  
213 lines have different reactions to RA, D3, and RA + D3 stimuli. RA, a current treatment  
214 for APL, is limited by RA resistance, variable efficacy in different cell types, and lack of  
215 understanding of the mechanism of action. Jensen *et al.*, studied transcriptional regu-  
216 lation in six leukemia cell lines to determine the changes in critical transcription factors  
217 in myelomonocytic differentiation between cell lines [50]. By using the experimental data  
218 from this study we wanted to find new network structures in each cell line and therefore,  
219 better understand the critical changes in the development of new cancer subtypes. The  
220 initial network structure curated from literature contained transcription factors as well as  
221 upstream markers for myelomonocytic lineage selection. Network perturbations included  
222 the addition and deletion of interactions as well as switching an interaction (i.e. upregu-  
223 lates to represses). We found new top network structures for all six cell lines and network  
224 perturbations can be found in Tables T5 - T10. Interestingly, there was no edge change  
225 that was consistent between all cell lines. Three network changes were made to five  
226 of six cell lines: switched or deleted AhR upregulates PU.1 (edge 100), added C/EBP $\alpha$   
227 upregulates VDR (edge 110), and switched or deleted C/EBP $\alpha$  upregulates PU.1 (edge  
228 118). Looking through the network perturbations we were able to find some literature  
229 evidence for a few interactions. For example upregulation of AP-1 by Oct1 was added to  
230 the network structure of four cell lines (K562, NB4, and WTHL60) and has been studied  
231 in [91]. This interaction was also added to the HL60 R38- model, except in this case AP-1  
232 was repressed by Oct1. By continuing to look through the data we can determine more

233 biologically relevant interactions found in the new models. The new leukemia cell line  
234 specific transcription factor models were able to improve the fit of experimental data from  
235 a subset of experiments. Some issues that need to be resolved include the fitting of many  
236 D3 only experiments.

237 The initial leukemia transcription factor network was assembled after extensive litera-  
238 ture review and hand curation of the biochemical interactions. One note was that interac-  
239 tions came from additional cell lines, including breast and prostate cancer, and therefore  
240 these interaction may or may not exist in leukemia cell lines. In this study we tried to  
241 determine new network structures by perturbing a best guess initial model network from  
242 literature. Data was limited to thirteen different proteins, out of 18 included in the model.  
243 Additional experiments with mRNA data would be useful in determining final model struc-  
244 tures as we modeled mRNA. A population study should be performed on the flow cytome-  
245 try data to see if population dynamics can be fit, not just single cell response. To improve  
246 the model network search a machine learning method could be used in which after each  
247 model perturbation error is calculated and based on this error a probability is given to the  
248 edges perturbed. For example, if we perturb edge ten and error triples, we can give the  
249 probability of making this step in the future very low. Also, it would be interesting to look  
250 at edges that have very little effect on model error. Another element that should be added  
251 to the model is the determination of granulocytic or monocytic differentiation in the cell  
252 lines in response to RA and D3 treatments. The ratio of PU.1 to C/EBPA $\alpha$  determines  
253 granulocytic vs. monocytic lineage selection [23]. CD38 and CD11b are myelomonocytic  
254 markers and CD14 is a monocytic specific marker. Overall the goal was to determine  
255 network structures to explain varying responses to RA and D3 treatment in six leukemia  
256 cell lines. The network structures found can be studied further to determine important  
257 functional changes between cell lines.

258 **Materials and Methods**

259 **0.3 Formulation of Network Model Equations** For each motif of N protein nodes, a  
260 mRNA and protein balance for each node is written as:

$$\frac{dm_j}{dt} = r_{X,j}v_{X,j} - k_{d,j}m_j - \mu m_j + \lambda \quad (1)$$

261

$$\frac{dp_j}{dt} = r_{T,j}v_{T,j} - k'_{d,j}p_j - \mu p_j \quad (2)$$

262 where  $j = 1, 2, 3 \dots N$ . Degradation rates are given as  $k_{d,j}$  and  $k'_{d,j}$ , and  $\lambda$  denotes a basal  
263 mRNA production rate.

264 The balances governing cellular infrastructure such as RNA polymerase (RNAP) and ri-  
265 bosomes (RIBO) are given by:

$$\frac{dRNAP}{dt} = (\alpha - RNAP)\mu \quad (3)$$

266

$$\frac{dRIBO}{dt} = (\beta - RIBO)\mu \quad (4)$$

267 where  $\alpha$  and  $\beta$  are constants. Balances governing a given inducer  $I_\pi$  and cellular growth  
268 rate  $\mu$ :

$$\frac{dI_z}{dt} = \delta \quad (5)$$

269

$$\frac{d\mu}{dt} = 0 \quad (6)$$

270 There are a total of  $2N + \Pi + 3$  differential equations for each motif, where  $\Pi$  is the number  
271 of inducers in the network.

272 The terms  $r_{X,j}$  and  $r_{T,j}$  denote the rate of transcription and translation respectively and  
273 are given by:

$$r_{X,j} = k_{X,j}(RNAP)\mu_j \quad (7)$$

274

$$r_{T,j} = k_{T,j}(RIBO)m_j\omega_j \quad (8)$$

275 where  $\mu_j$  and  $\omega_j$  describe the allocation of RNAP and RIBO resources to the expres-  
 276 sion and translation of node j:

$$\mu_j = k_{X,j}(RNAP) \left[ \sum_i k_{X,i}(RNAP) \right]^{-1} \quad (9)$$

277

$$\omega_j = k_{T,j}(RIBO)m_j \left[ \sum_i k_{T,i}(RIBO)m_i \right]^{-1} \quad (10)$$

278 The rate of expression and translation for node j is modified by control variables which  
 279 describe the regulatory inputs controlling the node. One assumption is that translation is  
 280 not actively regulated, thus  $v_{T,j} = 1$ . Transcription may be regulated by other proteins in  
 281 the motif. If the expression of species j had m activating factors and n repressive factors,  
 282 the control term was modeled as a mean:

$$v_j = \frac{\left( \sum_{i \in j^+} u_{i,j} + \sum_{i \in j^-} d_{i,j} \right)}{(m + n)} \quad (11)$$

283 where:

$$u_{ij} = f_{ij} \quad (12)$$

284

$$d_{ij} = 1 - f_{ij} \quad (13)$$

285 The quantities  $j^+$  and  $j^-$  denote the sets of activating and repressive factors for gene j.  
 286 There are many possible functional forms for  $0 \leq f_{ij}(\mathcal{Z}) \leq 1$ . Each individual transfer  
 287 function took the form:

$$f_i(x) = \frac{\kappa_{ij}^\eta \mathcal{Z}_j^\eta}{1 + \kappa_{ij}^\eta \mathcal{Z}_j^\eta} \quad (14)$$

288 where  $\mathcal{Z}_j$  denotes the abundance of the j factor (e.g. protein abundance), and  $\kappa_{i,j}$  and  $\eta$   
289 are control parameters. The  $\kappa_{i,j}$  parameter was a gain parameter and  $\eta$  was a coopera-  
290 tively parameter (similar to a Hill coefficient).

291 The small three protein network with one inducer contained 10 differential equations,  
292 20 control parameters, and 15 kinetic parameters. For the small three protein network  
293 the model equations were encoded using the Python programming language and solved  
294 using the ODEINT routine of the SciPy module [52]. The leukemia transcription factor  
295 network with two inducers (RA and D3), contained 42 differential equations (RXR was  
296 included but set to zero in this case), 652 control parameters, and 90 kinetic parameters.  
297 Due to the increased size of the network, the model equations in this case were encoded  
298 using the Julia programming language [10] and solved using the CVODE solver in the  
299 SUNDIALS library [45].

#### 300 **0.4 Estimation of top parameter sets using Particle Swarm Optimization (PSO)**

301 We used particle swarm optimization to estimate top parameter sets for each model.  
302 Particle swarm optimization employs a population of particles with their own coordinates,  
303 velocity and best fit error to find a global best fit error [34].

304 The mean squared error,  $\eta_j$ , of parameter set k for training objective  $j$  was defined as:

$$\eta_j(\mathbf{p}_k) = \frac{1}{N} \sum_i^N \frac{(\hat{x}_{i,j} - \beta_j x(\mathbf{p}_k)_{i,j})^2}{\hat{\sigma}_{i,j}^2} \quad (15)$$

305 The symbol  $\hat{x}_{i,j}$  denotes scaled experimental observations (from training objective j)  
306 while  $x(\mathbf{p}_k)_{i,j}$  denotes the simulation output (from training objective j). The quantity  $i$  de-  
307 notes the sampled time-index or condition, and  $N$  denotes the number of time points or  
308 conditions for experiment j. The standard deviation,  $\hat{\sigma}_{i,j}$ , was calculated from at least  
309 three experimental repeats.  $\beta_j$  is a scaling factor which is required when considering  
310 experimental data that is accurate only to a multiplicative constant. In this study, the

311 experimental data used for training and validation was typically band intensity from im-  
312 munoblots, where intensity was estimated using the ImageJ software package [1]. The  
313 scaling factor used was chosen to minimize the normalized squared error [12]:

$$\beta_j = \frac{\sum_i (\hat{x}_{i,j} x_{i,j} / \hat{\sigma}_{i,j}^2)}{\sum_i (x_{i,j} / \hat{\sigma}_{i,j})^2} \quad (16)$$

314 By using the scaling factor, the concentration units on simulation results were arbi-  
315 trary, which was consistent with the arbitrary units on the experimental training data. All  
316 simulation data was scaled by the corresponding  $\beta_j$ .

317 The cost function for the optimization problem can be expressed as:

$$\text{minimize } K(\mathbf{p}_k) = \sum_i^L \eta_j(\mathbf{p}_k) \quad (17)$$

318 where L is the number of objective functions used for training.

319 To begin PSO we randomly initialized a swarm of  $\mathcal{K}$ -dimensional particles (represented  
320 as  $\mathbf{x}_i$ ), which correspond to a  $\mathcal{K}$ -dimensional parameter vector. After running the neces-  
321 sary simulations, for each initial particle we calculated the particle error for all L objective  
322 functions, the total particle error (K), and the velocity vector (initially set to zero). Next we  
323 determined the global best error (i.e. the lowest K value for all particles) and global best  
324 particle position. For each operation after initialization, the velocity ( $\mathbf{v}_{i,j}$ ) and position ( $\mathbf{x}_{i,j}$ )  
325 of each particle were updated by the following equations:

$$\mathbf{v}_{i,j} = \theta \mathbf{v}_{i,j-1} + \mathcal{A} \mathbf{r}_1 (\mathcal{L}_i - \mathbf{x}_{i,j-1}) + \mathcal{B} \mathbf{r}_2 (\mathcal{G}\mathcal{L} - \mathbf{x}_{i,j-1}) \quad (18)$$

326

$$\mathbf{x}_{i,j} = \mathbf{x}_{i,j-1} + \mathbf{v}_{i,j} \quad (19)$$

327 where  $(\theta, \mathcal{A}, \mathcal{B})$  are adjustable parameters,  $\mathcal{L}_i$  denotes best local solution found by particle  
328  $i$  up until function evaluation  $j-1$ , and  $\mathcal{G}\mathcal{L}$  denotes the best global solution up until function

329 evaluation  $j - 1$ . The quantities  $\mathbf{r}_1$  and  $\mathbf{r}_2$  denotes uniform random vectors with the same  
330 dimension as the number of unknown model parameters ( $\mathcal{K}x1$ ).

331 Again for each new particle position we calculated the particle error for all L objective  
332 functions, the total particle error (K), and the velocity vector. Using a greedy search we  
updated  $\mathcal{L}_i$  and  $\mathcal{GL}$  by the following rules:

```
if  $K_{i,j} < K_{best,i}$  then
     $K_{best,i} = K_{i,j}$ 
     $\mathcal{L}_i = \mathbf{x}_{i,j}$ 
    if  $K_{i,j} < K_{globalbest}$  then
         $K_{globalbest} = K_{i,j}$ 
         $\mathcal{GL} = \mathbf{x}_{i,j}$ 
    end
end
```

333  
334 After J total operations we saved  $\mathcal{GL}$  and  $K_{globalbest}$  for the given model network struc-  
335 ture.

336 **References**

- 337 1. Abramoff M Magelhaes P RS (2004) Image processing with imagej. *Biophotonics Int*  
338 **11:** 36–42
- 339 2. Alon U (2007) *An introduction to systems biology: design principles of biological cir-*  
340 *cuits.* volume 10 of *Chapman & Hall/CRC mathematical and computational biology*  
341 *series.* Boca Raton, FL: Chapman & Hall/CRC
- 342 3. Altiok S, Xu M, Spiegelman BM (1997) PPARgamma induces cell cycle withdrawal:  
343 inhibition of E2F/DP DNA-binding activity via down-regulation of PP2A. *Genes Dev*  
344 **11:** 1987–98
- 345 4. Bailey JE (2001) Complex biology with no parameters. *Nat Biotechnol* **19:** 503–4
- 346 5. Balmer JE, Blomhoff R (2002) Gene expression regulation by retinoic acid. *J Lipid*  
347 *Res* **43:** 1773–808
- 348 6. Bauvois B, Durant L, Laboureau J, Barthélémy E, Rouillard D, Boulla G, Deterre P  
349 (1999) Upregulation of CD38 gene expression in leukemic B cells by interferon types  
350 I and II. *J Interferon Cytokine Res* **19:** 1059–66
- 351 7. Behre G, Whitmarsh AJ, Coghlan MP, Hoang T, Carpenter CL, Zhang DE, Davis RJ,  
352 Tenen DG (1999) c-Jun is a JNK-independent coactivator of the PU.1 transcription  
353 factor. *J Biol Chem* **274:** 4939–46
- 354 8. Ben-Shushan E, Sharir H, Pikarsky E, Bergman Y (1995) A dynamic balance between  
355 ARP-1/COUP-TFII, EAR-3/COUP-TFI, and retinoic acid receptor:retinoid X receptor  
356 heterodimers regulates Oct-3/4 expression in embryonal carcinoma cells. *Mol Cell*  
357 *Biol* **15:** 1034–48
- 358 9. Benkoussa M, Brand C, Delmotte MH, Formstecher P, Lefebvre P (2002) Retinoic acid  
359 receptors inhibit AP1 activation by regulating extracellular signal-regulated kinase and  
360 CBP recruitment to an AP1-responsive promoter. *Mol Cell Biol* **22:** 4522–34
- 361 10. Bezanson J, Edelman A, Karpinski S, Shah VB (2014) Julia: A Fresh Approach to

- 362 Numerical Computing
- 363 11. Bhatia M, Kirkland JB, Meckling-Gill KA (1994) M-CSF and 1,25 dihydroxy vitamin  
364 D3 synergize with 12-O-tetradecanoylphorbol-13-acetate to induce macrophage dif-  
365 ferentiation in acute promyelocytic leukemia NB4 cells. *Leukemia* **8**: 1744–9
- 366 12. Brown KS, Sethna JP (2003) Statistical mechanical approaches to models with many  
367 poorly known parameters. *Phys Rev E Stat Nonlin Soft Matter Phys* **68**: 021904
- 368 13. Bruemmer D, Yin F, Liu J, Berger JP, Sakai T, Blaschke F, Fleck E, Van Herle AJ, For-  
369 man BM, Law RE (2003) Regulation of the growth arrest and DNA damage-inducible  
370 gene 45 (GADD45) by peroxisome proliferator-activated receptor gamma in vascular  
371 smooth muscle cells. *Circ Res* **93**: e38–47
- 372 14. Bunaciu RP, Yen A (2011) Activation of the aryl hydrocarbon receptor AhR Promotes  
373 retinoic acid-induced differentiation of myeloblastic leukemia cells by restricting ex-  
374 pression of the stem cell transcription factor Oct4. *Cancer Res* **71**: 2371–80
- 375 15. Bunaciu RP, Yen A (2013) 6-Formylindolo (3,2-b)carbazole (FICZ) enhances retinoic  
376 acid (RA)-induced differentiation of HL-60 myeloblastic leukemia cells. *Mol Cancer*  
377 **12**: 39
- 378 16. Bushue N, Wan YJY (2010) Retinoid pathway and cancer therapeutics. *Adv Drug  
379 Deliv Rev* **62**: 1285–98
- 380 17. Chen F, Wang Q, Wang X, Studzinski GP (2004) Up-regulation of Egr1 by 1,25-  
381 dihydroxyvitamin D3 contributes to increased expression of p35 activator of cyclin-  
382 dependent kinase 5 and consequent onset of the terminal phase of HL60 cell differ-  
383 entiation. *Cancer Res* **64**: 5425–33
- 384 18. Chen H, Ray-Gallet D, Zhang P, Hetherington CJ, Gonzalez DA, Zhang DE, Moreau-  
385 Gachelin F, Tenen DG (1995) PU.1 (Spi-1) autoregulates its expression in myeloid  
386 cells. *Oncogene* **11**: 1549–60
- 387 19. Chen H, Zhang P, Radomska HS, Hetherington CJ, Zhang DE, Tenen DG (1996)

- 388 Octamer binding factors and their coactivator can activate the murine PU.1 (spi-1)  
389 promoter. *J Biol Chem* **271**: 15743–52
- 390 20. Cheung FSG, Lovicu FJ, Reichardt JKV (2012) Current progress in using vitamin D  
391 and its analogs for cancer prevention and treatment. *Expert Rev Anticancer Ther* **12**:  
392 811–37
- 393 21. Coombs CC, Tavakkoli M, Tallman MS (2015) Acute promyelocytic leukemia: where  
394 did we start, where are we now, and the future. *Blood Cancer J* **5**: e304
- 395 22. Dahl R, Iyer SR, Owens KS, Cuylear DD, Simon MC (2007) The transcriptional re-  
396 pressor GFI-1 antagonizes PU.1 activity through protein-protein interaction. *J Biol  
397 Chem* **282**: 6473–83
- 398 23. Dahl R, Walsh JC, Lancki D, Laslo P, Iyer SR, Singh H, Simon MC (2003) Regulation  
399 of macrophage and neutrophil cell fates by the PU.1:C/EBPalpha ratio and granulo-  
400 cyte colony-stimulating factor. *Nat Immunol* **4**: 1029–36
- 401 24. D'Alo' F, Johansen LM, Nelson EA, Radomska HS, Evans EK, Zhang P, Nerlov  
402 C, Tenen DG (2003) The amino terminal and E2F interaction domains are critical  
403 for C/EBP alpha-mediated induction of granulopoietic development of hematopoietic  
404 cells. *Blood* **102**: 3163–71
- 405 25. Dalton Jr WT, Ahearn MJ, McCredie KB, Freireich EJ, Stass SA, Trujillo JM (1988)  
406 HL-60 cell line was derived from a patient with FAB-M2 and not FAB-M3. *Blood* **71**:  
407 242–7
- 408 26. Defacque H, Commes T, Contet V, Sevilla C, Marti J (1995) Differentiation of U937  
409 myelomonocytic cell line by all-trans retinoic acid and 1,25-dihydroxyvitamin D3: syn-  
410 ergistic effects on tissue transglutaminase. *Leukemia* **9**: 1762–7
- 411 27. Delerive P, De Bosscher K, Besnard S, Vanden Berghe W, Peters JM, Gonzalez  
412 FJ, Fruchart JC, Tedgui A, Haegeman G, Staels B (1999) Peroxisome proliferator-  
413 activated receptor alpha negatively regulates the vascular inflammatory gene re-

- 414 sponse by negative cross-talk with transcription factors NF-kappaB and AP-1. *J Biol*  
415 *Chem* **274**: 32048–54
- 416 28. Dispirito JR, Fang B, Wang F, Lazar MA (2013) Pruning of the adipocyte peroxisome  
417 proliferator-activated receptor  $\gamma$  cistrome by hematopoietic master regulator PU.1.  
418 *Mol Cell Biol* **33**: 3354–64
- 419 29. Doan LL, Porter SD, Duan Z, Flubacher MM, Montoya D, Tsichlis PN, Horwitz M,  
420 Gilks CB, Grimes HL (2004) Targeted transcriptional repression of Gfi1 by GFI1 and  
421 GFI1B in lymphoid cells. *Nucleic Acids Res* **32**: 2508–19
- 422 30. Döhner H, Weisdorf DJ, Bloomfield CD (2015) Acute Myeloid Leukemia. *N Engl J*  
423 *Med* **373**: 1136–52
- 424 31. Drach J, McQueen T, Engel H, Andreeff M, Robertson KA, Collins SJ, Malavasi F,  
425 Mehta K (1994) Retinoic acid-induced expression of CD38 antigen in myeloid cells is  
426 mediated through retinoic acid receptor-alpha. *Cancer Res* **54**: 1746–52
- 427 32. Duan Z, Horwitz M (2003) Targets of the transcriptional repressor oncoprotein Gfi-1.  
428 *Proc Natl Acad Sci U S A* **100**: 5932–7
- 429 33. Dunlop TW, Väisänen S, Frank C, Molnár F, Sinkkonen L, Carlberg C (2005) The  
430 human peroxisome proliferator-activated receptor delta gene is a primary target of  
431 1alpha,25-dihydroxyvitamin D3 and its nuclear receptor. *J Mol Biol* **349**: 248–60
- 432 34. Eberhart RC, Kennedy J (1995) A new optimizer using particle swarm theory. *Pro-*  
433 *ceedings of the Sixth International Symposium on Micro Machine and Human Sci-*  
434 *ence* : 39–43
- 435 35. Fei J, Cook C, Gillespie M, Yu B, Fullen K, Santanam N (2011) Atherogenic  $\omega$ -6 Lipids  
436 Modulate PPAR- EGR-1 Crosstalk in Vascular Cells. *PPAR Res* **2011**: 753917
- 437 36. Fontana JA, Colbert DA, Deisseroth AB (1981) Identification of a population of bipo-  
438 tent stem cells in the HL60 human promyelocytic leukemia cell line. *Proc Natl Acad*  
439 *Sci U S A* **78**: 3863–6

- 440 37. Friedman AD (2002) Transcriptional regulation of myelopoiesis. *Int J Hematol* **75**:  
441 466–72
- 442 38. Friedman AD (2007) Transcriptional control of granulocyte and monocyte develop-  
443 ment. *Oncogene* **26**: 6816–28
- 444 39. Fu M, Zhang J, Lin Y, Zhu X, Ehrengruber MU, Chen YE (2002) Early growth  
445 response factor-1 is a critical transcriptional mediator of peroxisome proliferator-  
446 activated receptor-gamma 1 gene expression in human aortic smooth muscle cells. *J  
447 Biol Chem* **277**: 26808–14
- 448 40. Göbel F, Taschner S, Jurkin J, Konradi S, Vaculik C, Richter S, Kneidinger D,  
449 Mühlbacher C, Bieglmayer C, Elbe-Bürger A, Strobl H (2009) Reciprocal role of GATA-  
450 1 and vitamin D receptor in human myeloid dendritic cell differentiation. *Blood* **114**:  
451 3813–21
- 452 41. Gocek E, Marchwicka A, Baurska H, Chrobak A, Marcinkowska E (2012) Opposite  
453 regulation of vitamin D receptor by ATRA in AML cells susceptible and resistant to  
454 vitamin D-induced differentiation. *J Steroid Biochem Mol Biol* **132**: 220–6
- 455 42. Han S, Sidell N, Fisher PB, Roman J (2004) Up-regulation of p21 gene expression  
456 by peroxisome proliferator-activated receptor gamma in human lung carcinoma cells.  
457 *Clin Cancer Res* **10**: 1911–9
- 458 43. Harris TE, Albrecht JH, Nakanishi M, Darlington GJ (2001) CCAAT/enhancer-binding  
459 protein-alpha cooperates with p21 to inhibit cyclin-dependent kinase-2 activity and  
460 induces growth arrest independent of DNA binding. *J Biol Chem* **276**: 29200–9
- 461 44. Hasemann MS, Lauridsen FKB, Waage J, Jakobsen JS, Frank AK, Schuster MB,  
462 Rapin N, Bagger FO, Hoppe PS, Schroeder T, Porse BT (2014) C/EBP $\alpha$  is required  
463 for long-term self-renewal and lineage priming of hematopoietic stem cells and for the  
464 maintenance of epigenetic configurations in multipotent progenitors. *PLoS Genet* **10**:  
465 e1004079

- 466 45. Hindmarsh A, Brown P, Grant K, Lee S, Serban R, Shumaker D, Woodward C (2005)  
467       SUNDIALS: Suite of nonlinear and differential/algebraic equation solvers. *ACM Trans-*  
468       *actions on Mathematical Software* **31**: 363–396
- 469 46. Hunger SP, Mullighan CG (2015) Acute Lymphoblastic Leukemia in Children. *N Engl*  
470       *J Med* **373**: 1541–52
- 471 47. Jabbour E, Kantarjian H (2014) Chronic myeloid leukemia: 2014 update on diagnosis,  
472       monitoring, and management. *Am J Hematol* **89**: 547–56
- 473 48. Jensen HA, Bunaciu RP, Ibabao CN, Myers R, Varner JD, Yen A (2014) Retinoic acid  
474       therapy resistance progresses from unilineage to bilineage in HL-60 leukemic blasts.  
475       *PLoS One* **9**: e98929
- 476 49. Jensen HA, Styskal LE, Tassey R, Bunaciu RP, Congleton J, Varner JD, Yen A (2013)  
477       The Src-family kinase inhibitor PP2 rescues inducible differentiation events in emer-  
478       gent retinoic acid-resistant myeloblastic leukemia cells. *PLoS One* **8**: e58621
- 479 50. Jensen HA, Yourish HB, Bunaciu RP, Varner JD, Yen A (2015) Induced myelomono-  
480       cytic differentiation in leukemia cells is accompanied by noncanonical transcription  
481       factor expression. *FEBS Open Bio* **5**: 789–800
- 482 51. Johnson DG, Ohtani K, Nevins JR (1994) Autoregulatory control of E2F1 expression  
483       in response to positive and negative regulators of cell cycle progression. *Genes Dev*  
484       **8**: 1514–25
- 485 52. Jones E, Oliphant T, Peterson P (2001) SciPy: Open source scientific tools for Python
- 486 53. Kakizawa T, Miyamoto T, Ichikawa K, Kaneko A, Suzuki S, Hara M, Nagasawa T,  
487       Takeda T, Mori Ji, Kumagai M, Hashizume K (1999) Functional interaction between  
488       Oct-1 and retinoid X receptor. *J Biol Chem* **274**: 19103–8
- 489 54. Kardassis D, Papakosta P, Pardali K, Moustakas A (1999) c-Jun transactivates the  
490       promoter of the human p21(WAF1/Cip1) gene by acting as a superactivator of the  
491       ubiquitous transcription factor Sp1. *J Biol Chem* **274**: 29572–81

- 492 55. Kholodenko B, Yaffe MB, Kolch W (2012) Computational approaches for analyzing  
493 information flow in biological networks. *Sci Signal* **5**: re1
- 494 56. Laslo P, Spooner CJ, Warmflash A, Lancki DW, Lee HJ, Sciammas R, Gantner BN,  
495 Dinner AR, Singh H (2006) Multilineage transcriptional priming and determination of  
496 alternate hematopoietic cell fates. *Cell* **126**: 755–66
- 497 57. Li SL, Schlegel W, Valente AJ, Clark RA (1999) Critical flanking sequences of PU.1  
498 binding sites in myeloid-specific promoters. *J Biol Chem* **274**: 32453–60
- 499 58. Lidonnici MR, Audia A, Soliera AR, Prisco M, Ferrari-Amorotti G, Waldron T, Do-  
500 nato N, Zhang Y, Martinez RV, Holyoake TL, Calabretta B (2010) Expression of the  
501 transcriptional repressor Gfi-1 is regulated by C/EBPalpha and is involved in its pro-  
502 liferation and colony formation-inhibitory effects in p210BCR/ABL-expressing cells.  
503 *Cancer Res* **70**: 7949–59
- 504 59. Liu M, Freedman LP (1994) Transcriptional synergism between the vitamin D3 recep-  
505 tor and other nonreceptor transcription factors. *Mol Endocrinol* **8**: 1593–604
- 506 60. Liu M, Iavarone A, Freedman LP (1996) Transcriptional activation of the human  
507 p21(WAF1/CIP1) gene by retinoic acid receptor. Correlation with retinoid induction  
508 of U937 cell differentiation. *J Biol Chem* **271**: 31723–8
- 509 61. Liu M, Lee MH, Cohen M, Bommakanti M, Freedman LP (1996) Transcriptional ac-  
510 tivation of the Cdk inhibitor p21 by vitamin D3 leads to the induced differentiation of  
511 the myelomonocytic cell line U937. *Genes Dev* **10**: 142–53
- 512 62. Lozzio CB, Lozzio BB (1975) Human chronic myelogenous leukemia cell-line with  
513 positive Philadelphia chromosome. *Blood* **45**: 321–34
- 514 63. Luo XM, Ross AC (2006) Retinoic acid exerts dual regulatory actions on the expres-  
515 sion and nuclear localization of interferon regulatory factor-1. *Exp Biol Med Maywood*  
516 **231**: 619–31
- 517 64. Mak KS, Funnell APW, Pearson RCM, Crossley M (2011) PU.1 and Haematopoietic

- 518 Cell Fate: Dosage Matters. *Int J Cell Biol* **2011**: 808524
- 519 65. Marlowe JL, Knudsen ES, Schwemberger S, Puga A (2004) The aryl hydrocarbon  
520 receptor displaces p300 from E2F-dependent promoters and represses S phase-  
521 specific gene expression. *J Biol Chem* **279**: 29013–22
- 522 66. Martinez JM, Baek SJ, Mays DM, Tithof PK, Eling TE, Walker NJ (2004) EGR1 is a  
523 novel target for AhR agonists in human lung epithelial cells. *Toxicol Sci* **82**: 429–35
- 524 67. Mueller BU, Pabst T, Fos J, Petkovic V, Fey MF, Asou N, Buergi U, Tenen DG (2006)  
525 ATRA resolves the differentiation block in t(15;17) acute myeloid leukemia by restoring  
526 PU.1 expression. *Blood* **107**: 3330–8
- 527 68. Munker R, Norman A, Koeffler HP (1986) Vitamin D compounds. Effect on clonal  
528 proliferation and differentiation of human myeloid cells. *J Clin Invest* **78**: 424–30
- 529 69. Nabhan C, Rosen ST (2014) Chronic lymphocytic leukemia: a clinical review. *JAMA*  
530 **312**: 2265–76
- 531 70. Nakajima H, Kizaki M, Ueno H, Muto A, Takayama N, Matsushita H, Sonoda A, Ikeda  
532 Y (1996) All-trans and 9-cis retinoic acid enhance 1,25-dihydroxyvitamin D3-induced  
533 monocytic differentiation of U937 cells. *Leuk Res* **20**: 665–76
- 534 71. Olsson IL, Breitman TR (1982) Induction of differentiation of the human histiocytic  
535 lymphoma cell line U-937 by retinoic acid and cyclic adenosine 3':5'-monophosphate-  
536 inducing agents. *Cancer Res* **42**: 3924–7
- 537 72. Pahl HL, Scheibe RJ, Zhang DE, Chen HM, Galson DL, Maki RA, Tenen DG (1993)  
538 The proto-oncogene PU.1 regulates expression of the myeloid-specific CD11b pro-  
539 moter. *J Biol Chem* **268**: 5014–20
- 540 73. Pan Z, Hetherington CJ, Zhang DE (1999) CCAAT/enhancer-binding protein activates  
541 the CD14 promoter and mediates transforming growth factor beta signaling in mono-  
542 cyte development. *J Biol Chem* **274**: 23242–8
- 543 74. Pankratova EV, Sytina EV, Luchina NN, Krivega IV (2003) The regulation of the Oct-1

- 544 gene transcription is mediated by two promoters. *Immunol Lett* **88**: 15–20
- 545 75. Passioura T, Dolnikov A, Shen S, Symonds G (2005) N-ras-induced growth suppression  
546 of myeloid cells is mediated by IRF-1. *Cancer Res* **65**: 797–804
- 547 76. Rishi AK, Gerald TM, Shao ZM, Li XS, Baumann RG, Dawson MI, Fontana JA (1996)  
548 Regulation of the human retinoic acid receptor alpha gene in the estrogen receptor  
549 negative human breast carcinoma cell lines SKBR-3 and MDA-MB-435. *Cancer Res*  
550 **56**: 5246–52
- 551 77. Robertson KA, Mueller L, Collins SJ (1991) Retinoic acid receptors in myeloid  
552 leukemia: characterization of receptors in retinoic acid-resistant K-562 cells. *Blood*  
553 **77**: 340–7
- 554 78. Rosen ED, Hsu CH, Wang X, Sakai S, Freeman MW, Gonzalez FJ, Spiegelman BM  
555 (2002) C/EBPalpha induces adipogenesis through PPARgamma: a unified pathway.  
556 *Genes Dev* **16**: 22–6
- 557 79. Sadeghi K, Wessner B, Laggner U, Ploder M, Tamandl D, Friedl J, Zügel U, Stein-  
558 meyer A, Pollak A, Roth E, Boltz-Nitulescu G, Spittler A (2006) Vitamin D3 down-  
559 regulates monocyte TLR expression and triggers hyporesponsiveness to pathogen-  
560 associated molecular patterns. *Eur J Immunol* **36**: 361–70
- 561 80. Shen M, Bunaciu RP, Congleton J, Jensen HA, Sayam LG, Varner JD, Yen A (2011)  
562 Interferon regulatory factor-1 binds c-Cbl, enhances mitogen activated protein kinase  
563 signaling and promotes retinoic acid-induced differentiation of HL-60 human myelo-  
564 monoblastic leukemia cells. *Leuk Lymphoma* **52**: 2372–9
- 565 81. Shen Q, Uray IP, Li Y, Krisko TI, Strecker TE, Kim HT, Brown PH (2008) The AP-1  
566 transcription factor regulates breast cancer cell growth via cyclins and E2F factors.  
567 *Oncogene* **27**: 366–77
- 568 82. Siegel RL, Miller KD, Jemal A (2015) Cancer statistics, 2015. *CA Cancer J Clin* **65**:  
569 5–29

- 570 83. Song EK, Lee YR, Kim YR, Yeom JH, Yoo CH, Kim HK, Park HM, Kang HS, Kim  
571 JS, Kim UH, Han MK (2012) NAADP mediates insulin-stimulated glucose uptake and  
572 insulin sensitization by PPAR $\gamma$  in adipocytes. *Cell Rep* **2**: 1607–19
- 573 84. Steidl U, Rosenbauer F, Verhaak RGW, Gu X, Ebralidze A, Otu HH, Klippel S, Steidl C,  
574 Bruns I, Costa DB, Wagner K, Aivado M, Kobbe G, Valk PJM, Passegue E, Libermann  
575 TA, Delwel R, Tenen DG (2006) Essential role of Jun family transcription factors in  
576 PU.1 knockdown-induced leukemic stem cells. *Nat Genet* **38**: 1269–77
- 577 85. Suh J, Jeon YJ, Kim HM, Kang JS, Kaminski NE, Yang KH (2002) Aryl hydrocarbon  
578 receptor-dependent inhibition of AP-1 activity by 2,3,7,8-tetrachlorodibenzo-p-dioxin  
579 in activated B cells. *Toxicol Appl Pharmacol* **181**: 116–23
- 580 86. Sylvester I, Schöler HR (1994) Regulation of the Oct-4 gene by nuclear receptors.  
581 *Nucleic Acids Res* **22**: 901–11
- 582 87. Szanto A, Nagy L (2005) Retinoids potentiate peroxisome proliferator-activated re-  
583 ceptor gamma action in differentiation, gene expression, and lipid metabolic pro-  
584 cesses in developing myeloid cells. *Mol Pharmacol* **67**: 1935–43
- 585 88. Tang XH, Gudas LJ (2011) Retinoids, retinoic acid receptors, and cancer. *Annu Rev*  
586 *Pathol* **6**: 345–64
- 587 89. Testa U, Grignani F, Barberi T, Fagioli M, Masciulli R, Ferrucci PF, Seripa D, Camagna  
588 A, Alcalay M, Pelicci PG (1994) PML/RAR alpha+ U937 mutant and NB4 cell lines:  
589 retinoic acid restores the monocytic differentiation response to vitamin D3. *Cancer*  
590 *Res* **54**: 4508–15
- 591 90. Timchenko N, Wilson DR, Taylor LR, Abdelsayed S, Wilde M, Sawadogo M, Dar-  
592 lington GJ (1995) Autoregulation of the human C/EBP alpha gene by stimulation of  
593 upstream stimulatory factor binding. *Mol Cell Biol* **15**: 1192–202
- 594 91. Ullman KS, Northrop JP, Admon A, Crabtree GR (1993) Jun family members are con-  
595 trolled by a calcium-regulated, cyclosporin A-sensitive signaling pathway in activated

- 596 T lymphocytes. *Genes Dev* **7**: 188–96
- 597 92. Varley CL, Bacon EJ, Holder JC, Southgate J (2009) FOXA1 and IRF-1 intermediary  
598 transcriptional regulators of PPARgamma-induced urothelial cytodifferentiation. *Cell  
599 Death Differ* **16**: 103–14
- 600 93. Villaverde AF, Banga JR (2014) Reverse engineering and identification in systems  
601 biology: strategies, perspectives and challenges. *J R Soc Interface* **11**: 20130505
- 602 94. Von Knethen A, Brüne B (2002) Activation of peroxisome proliferator-activated recep-  
603 tor gamma by nitric oxide in monocytes/macrophages down-regulates p47phox and  
604 attenuates the respiratory burst. *J Immunol* **169**: 2619–26
- 605 95. Wang N, Verna L, Chen NG, Chen J, Li H, Forman BM, Stemerman MB (2002) Con-  
606 stitutive activation of peroxisome proliferator-activated receptor-gamma suppresses  
607 pro-inflammatory adhesion molecules in human vascular endothelial cells. *J Biol  
608 Chem* **277**: 34176–81
- 609 96. Widerak M, Ghoneim C, Dumontier MF, Quesne M, Corvol MT, Savouret JF (2006)  
610 The aryl hydrocarbon receptor activates the retinoic acid receptoralpha through  
611 SMRT antagonism. *Biochimie* **88**: 387–97
- 612 97. Wu W, Zhang X, Zanello LP (2007) 1alpha,25-Dihydroxyvitamin D(3) antiproliferative  
613 actions involve vitamin D receptor-mediated activation of MAPK pathways and AP-  
614 1/p21(waf1) upregulation in human osteosarcoma. *Cancer Lett* **254**: 75–86
- 615 98. Yuki H, Ueno S, Tatetsu H, Niilo H, Iino T, Endo S, Kawano Y, Komohara Y, Takeya  
616 M, Hata H, Okada S, Watanabe T, Akashi K, Mitsuya H, Okuno Y (2013) PU.1 is a  
617 potent tumor suppressor in classical Hodgkin lymphoma cells. *Blood* **121**: 962–70
- 618 99. Zaragoza K, Bégay V, Schuetz A, Heinemann U, Leutz A (2010) Repression of tran-  
619 scriptional activity of C/EBPalpha by E2F-dimerization partner complexes. *Mol Cell  
620 Biol* **30**: 2293–304

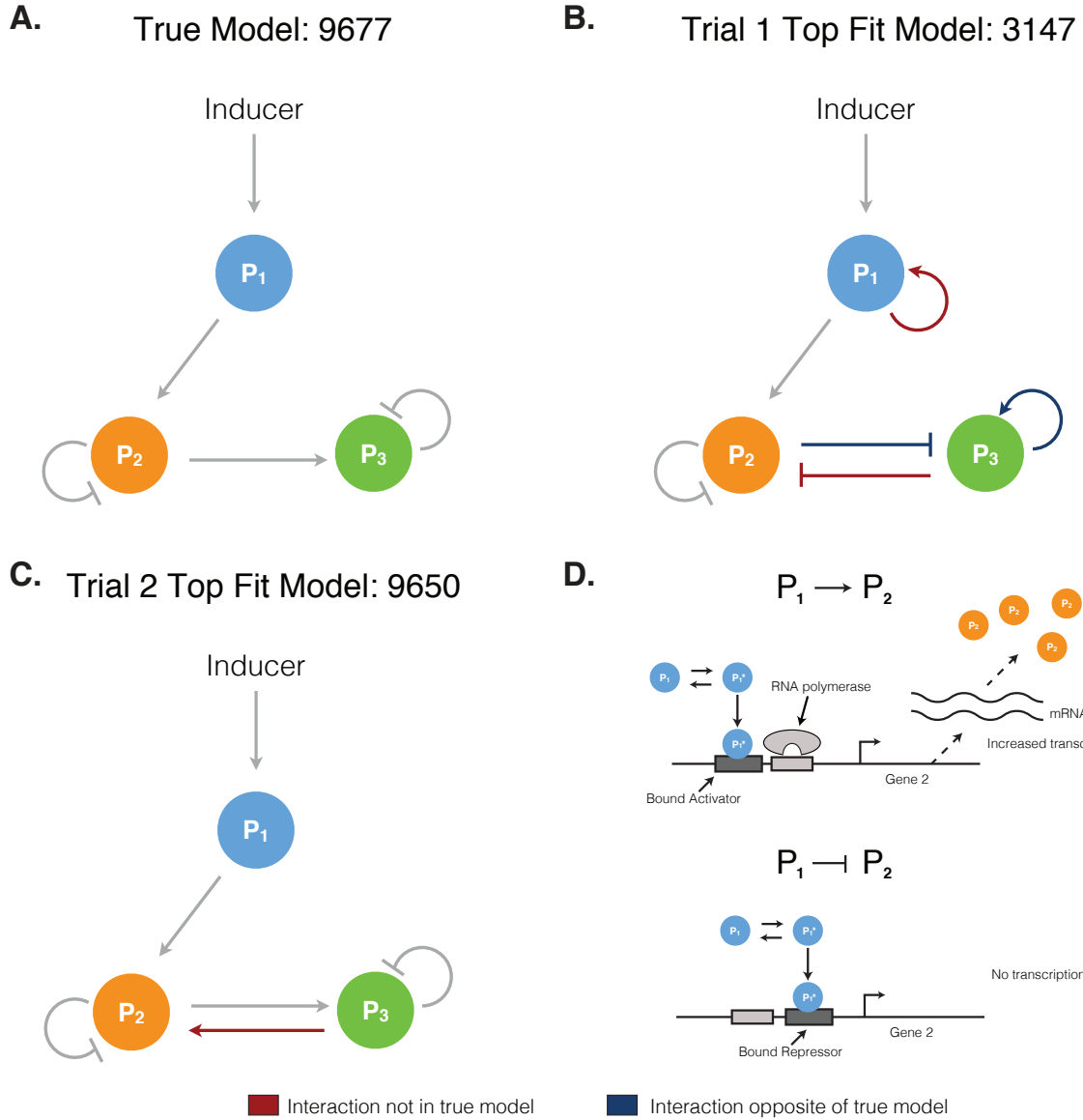


**Fig. 1:** Model for three node protein network. Arrows denote activation and lines denote inhibition. The model includes three proteins ( $P_1$ ,  $P_2$ , and  $P_3$ ), the corresponding mRNA ( $mRNA_1$ ,  $mRNA_2$ , and  $mRNA_3$ ), RNA polymerase (RNAP), ribosomes (RIBO), and Inducer. **A.** The true model for the three node protein network. **B.** The best fit model after parameter estimation using data from only one experiment. **C.** The best fit model after parameter estimation using data from experiments 1, 2 and 3. Red lines denote interactions not in original model and blue lines denote interactions that are opposite of the original model. **D.** Gene transcription activation and repression in the model (figure modified from [2]).

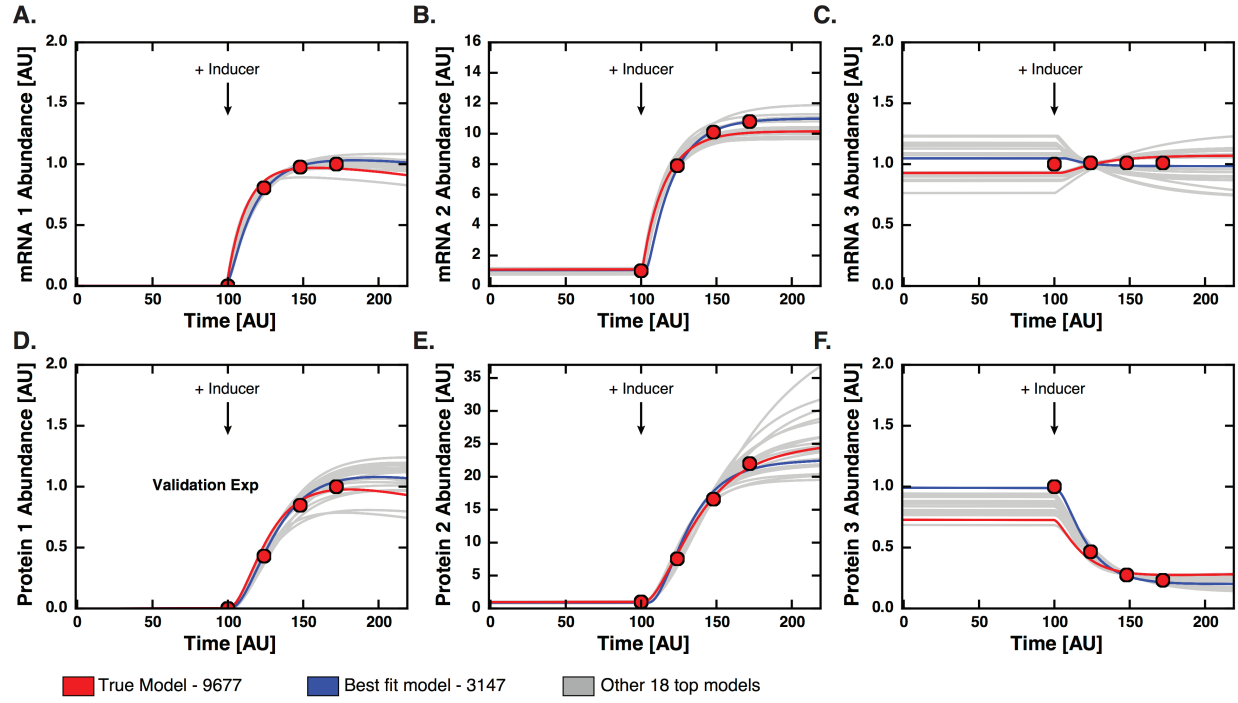


**Fig. 2:** Experiment 1 results for the top 20 models with respective best parameter sets determined from particle swarm optimization. In experiment 1, inducer was added at Time = 100. **A, B, C.** Plots of mRNA concentration profiles for species 1, 2, and 3 after inducer added at Time = 100. **D.** Plot of protein concentration profile for species 1 which was used for validation. **E, F.** Plots of protein concentration profiles for species 2 and 3. Red dots denote synthetic experimental data used for fitting. Red lines represent the true model with optimized parameters, blue denotes the best fitting model (1B), and the grey lines represent remaining top 18 models.

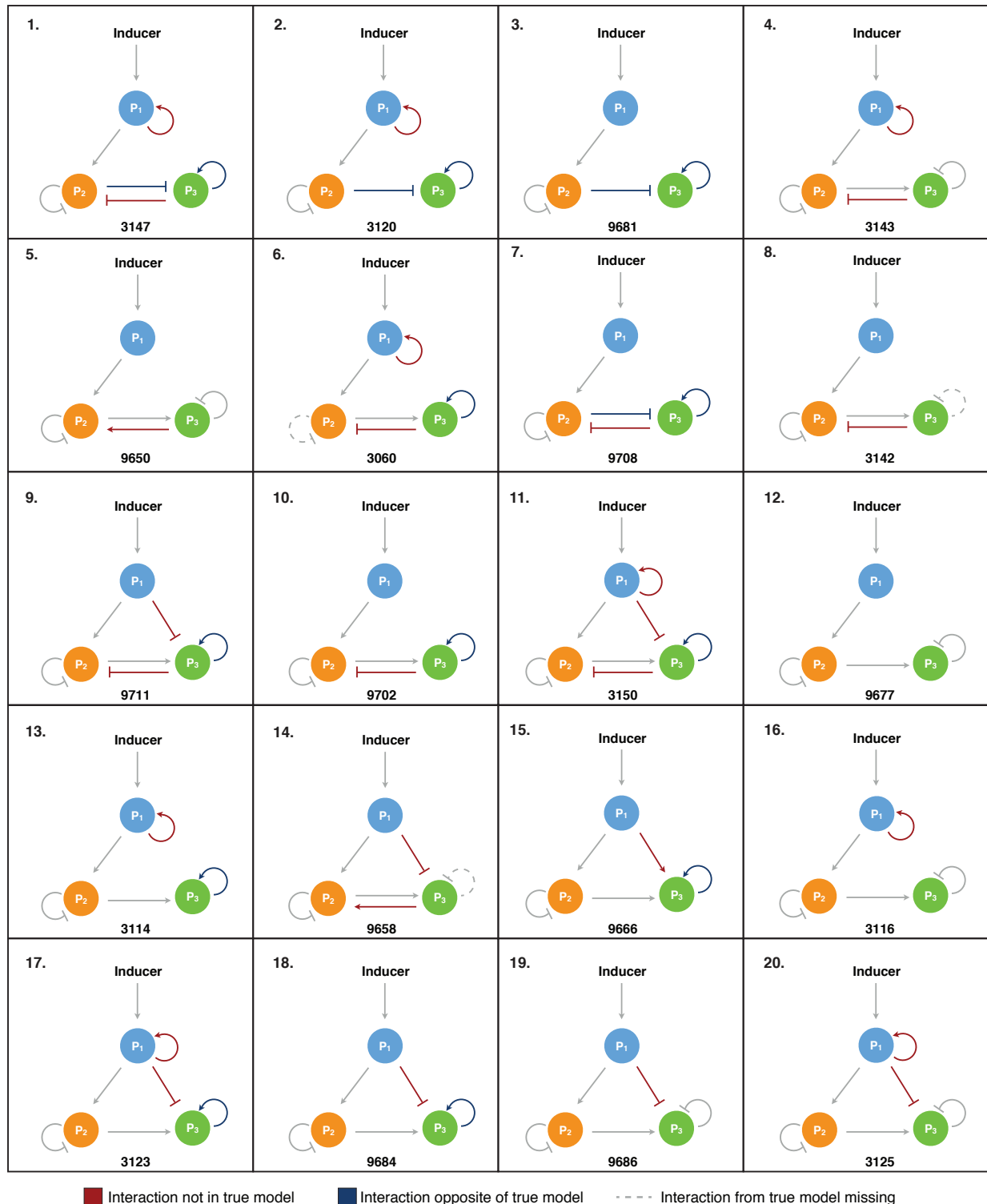


**Fig. 3:** Structures of top 20 three protein node models. Models are arranged from lowest error (best fit) to highest error, with the true model at number 12. Red denotes interactions not in original model, blue denotes interactions that are opposite of the original model, and dotted lines denote interactions in true model that are missing in structure. Numbers (i.e. 3147) denote the specific model number out of the total 19683 structures.

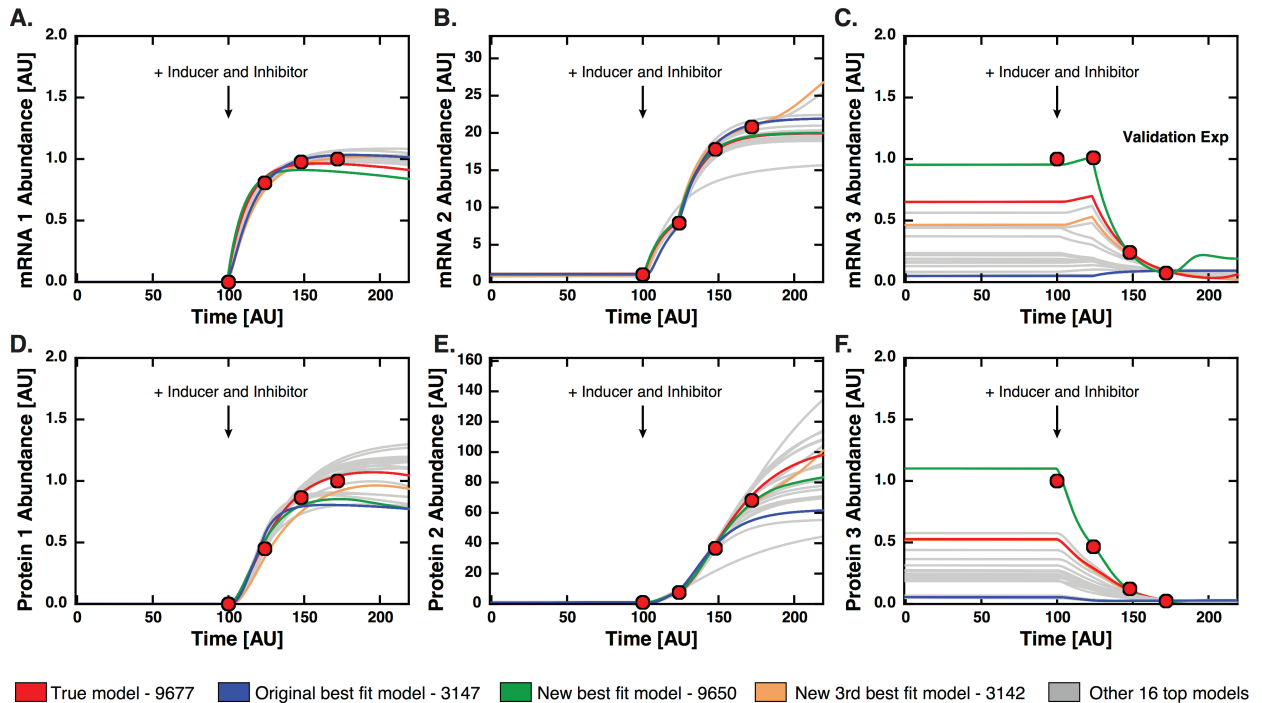
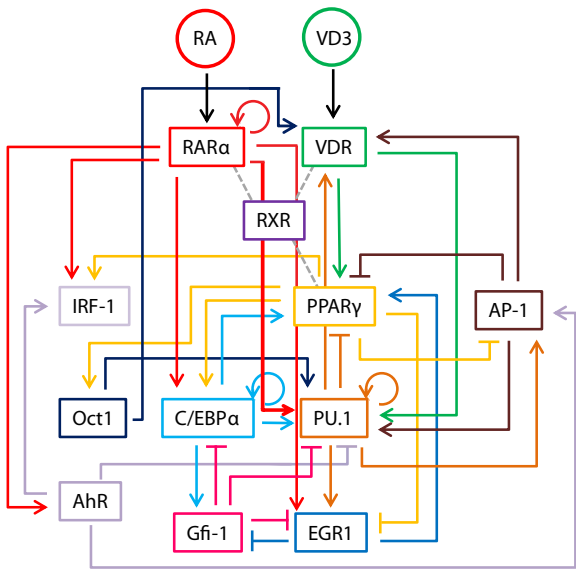


**Fig. 4:** Experiment 2 results for the top 20 models with respective best parameter sets determined from particle swarm optimization. In experiment 2, inducer and an inhibitor for  $P_2$  were added at Time = 100. **A, B.** Plots of mRNA concentration profiles for species 1 and 2 after inducer and inhibitor added at Time = 100. **C.** Plot of mRNA concentration profile for species 3 which was used for validation. **D, E, F.** Plots of protein concentration profiles for species 1, 2, and 3. Red dots denote synthetic experimental data used for fitting. Red lines represent the true model with new optimized parameters, blue denotes the best fitting model after experiment 1 (1B), green denotes the new best fitting model, orange denotes the third best fit model, and the grey lines represent remaining top 18 models.

### Transcription Factor Network



### Phenotypic Markers

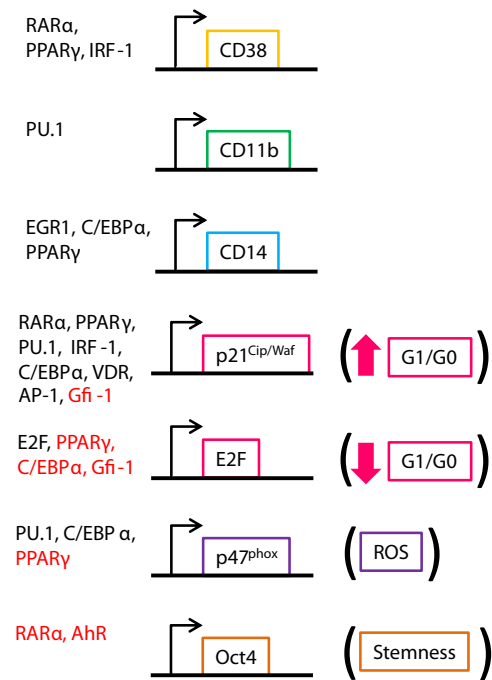


**Fig. 5:** Initial myelomonocytic transcription factor network structure from literature sources. Figure shows interactions between protein nodes with arrows indicating transcriptional activation and lines indicating transcriptional repression. Phenotypic markers are shown on the right side, with black indicating activation and red repression. RXR (shown in the figure) was assumed to exist in an active form to dimerize with RAR $\alpha$ , VDR, and PPAR $\gamma$  and was excluded in this network identification problem.

**Table 1:** Initial myelomonocytic transcription factor network list with transcription factor, effect, target gene, and reference

Transcription Factor	General Effect	Target Gene	Reference(s)
RAR $\alpha$	upregulates	RAR $\alpha$	[76]
RAR $\alpha$	upregulates	PU.1	[67]
RAR $\alpha$	upregulates	C/EBP $\alpha$	[38]
RAR $\alpha$	upregulates	IRF-1	[63]
RAR $\alpha$	represses	Oct4	[86]
RAR $\alpha$	upregulates	CD38	[31]
RAR $\alpha$	upregulates	p21	[60]
RAR $\alpha$	upregulates	AhR	[15]
RAR $\alpha$	upregulates	EGR1	[5]
VDR	upregulates	PPAR $\gamma$	[33]
VDR	upregulates	PU.1	
VDR	upregulates	p21	[61]
PPAR $\gamma$	upregulates	C/EBP $\alpha$	[78]
PPAR $\gamma$	upregulates	IRF-1	[92]
PPAR $\gamma$	upregulates	Oct1	[13]
PPAR $\gamma$	represses	AP-1	[27]
PPAR $\gamma$	represses	E2F	[3]
PPAR $\gamma$	represses	EGR1	[35]
PPAR $\gamma$	upregulates	CD38	[83]
PPAR $\gamma$	upregulates	CD14	[87]
PPAR $\gamma$	upregulates	p21	[42]
PPAR $\gamma$	represses	p47phox	[94]
PU.1	represses	PPAR $\gamma$	[28]
PU.1	upregulates	PU.1	[18]
PU.1	upregulates	AP-1	[84]
PU.1	upregulates	EGR1	[56]
PU.1	upregulates	CD11b	[72]
PU.1	upregulates	p21	[98]
PU.1	upregulates	p47phox	[57]
PU.1	upregulates	VDR	[40]
C/EBP $\alpha$	upregulates	PPAR $\gamma$	[78]
C/EBP $\alpha$	upregulates	PU.1	[23]
C/EBP $\alpha$	upregulates	C/EBP $\alpha$	[90]
C/EBP $\alpha$	upregulates	Gfi-1	[58]
C/EBP $\alpha$	represses	E2F	[24]
C/EBP $\alpha$	upregulates	CD14	[73]
C/EBP $\alpha$	upregulates	p21	[43]
IRF-1	upregulates	CD38	[6]
IRF-1	upregulates	p21	[75]
Gfi-1	represses	PU.1	[22]
Gfi-1	represses	C/EBP $\alpha$	[32]

623	Gfi-1	represses	E2F	[32]
	Gfi-1	represses	EGR1	[56]
	Gfi-1	represses	p21	[32]
	Oct1	upregulates	VDR	[59]
	Oct1	upregulates	PU.1	[19]
	AP-1	upregulates	VDR	[59]
	AP-1	represses	PPAR $\gamma$	[27]
	AP-1	upregulates	PU.1	[7]
	AP-1	upregulates	p21	[54]
	E2F	upregulates	E2F	[51]
	EGR1	upregulates	PPAR $\gamma$	[39]
	EGR1	represses	Gfi-1	[64]
	EGR1	upregulates	CD14	[17]
	AhR	upregulates	AP-1	[85]
	AhR	upregulates	IRF-1	[80]
	AhR	represses	Oct4	[14]
	AhR	represses	PU.1	

## HL60 R38-

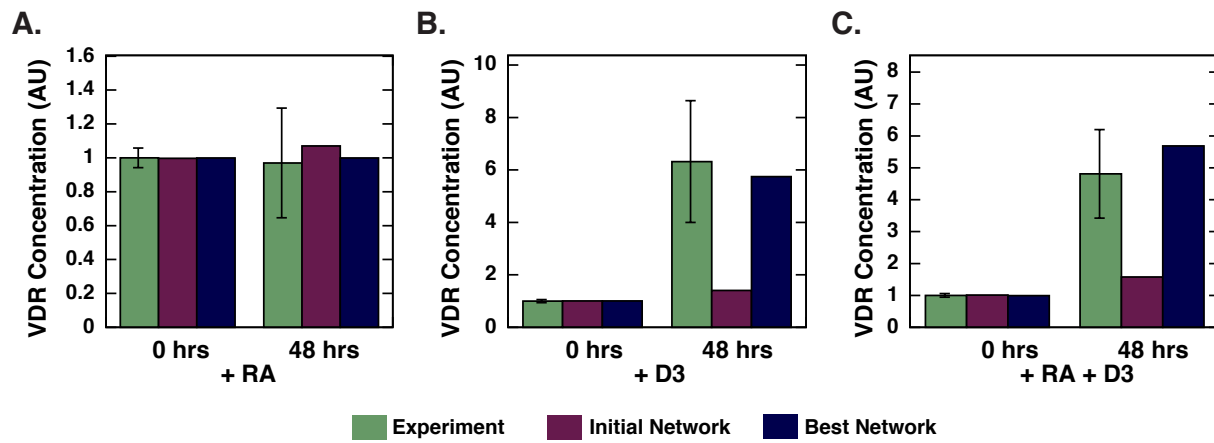


**Fig. 6:** Selected training results for the HL60 R38- cell line. A., B., C. Simulation and experimental results of change in VDR concentration due to RA, D3, and RA/D3 stimulus, respectively. Green denotes experimental data, pink denotes simulation data from the initial network, and blue denotes simulation data from the best network. The top parameter set is used, and error bars denote standard experimental error.

## HL60

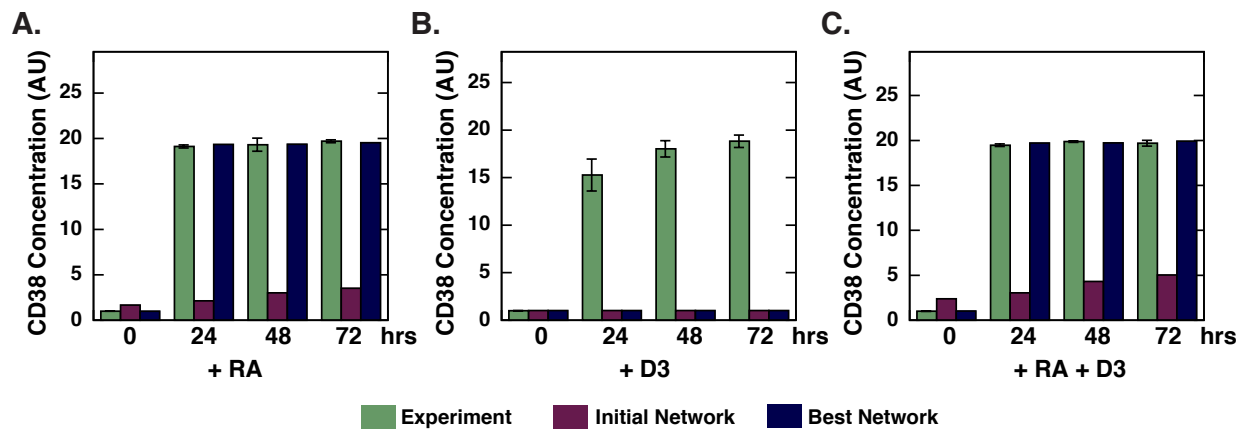


**Fig. 7:** Selected training results for the HL60 cell line. A., B., C. Simulation and experimental results of change in cells expressing CD38 due to RA, D3, and RA/D3 stimulus, respectively. Green denotes experimental data, pink denotes simulation data from the initial network, and blue denotes simulation data from the best network. The top parameter set is used, and error bars denote standard experimental error.

## NB4

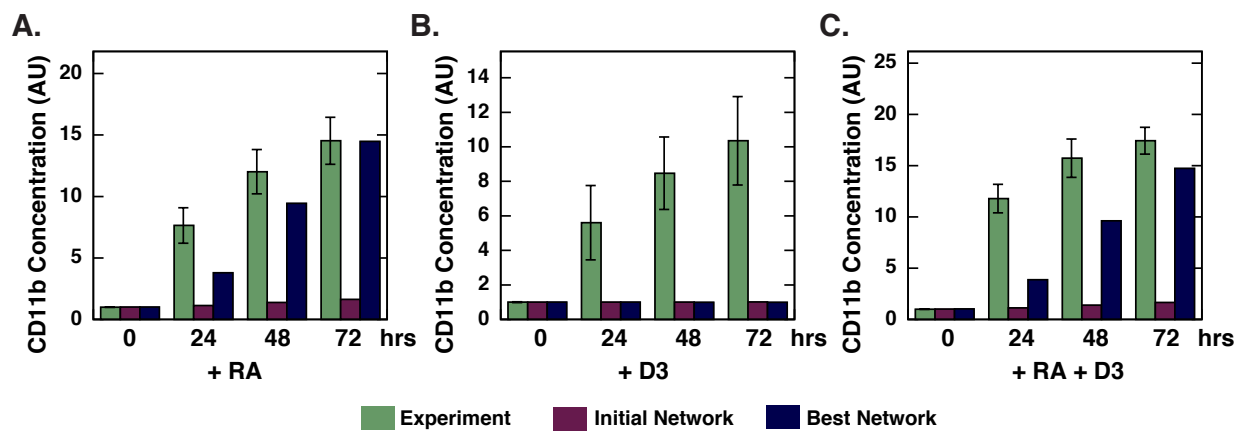


**Fig. 8:** Selected training results for the NB4 cell line. A., B., C. Simulation and experimental results of change in CD11b concentration due to RA, D3, and RA/D3 stimulus, respectively. Green denotes experimental data, pink denotes simulation data from the initial network, and blue denotes simulation data from the best network. The top parameter set is used, and error bars denote standard experimental error.

## K562

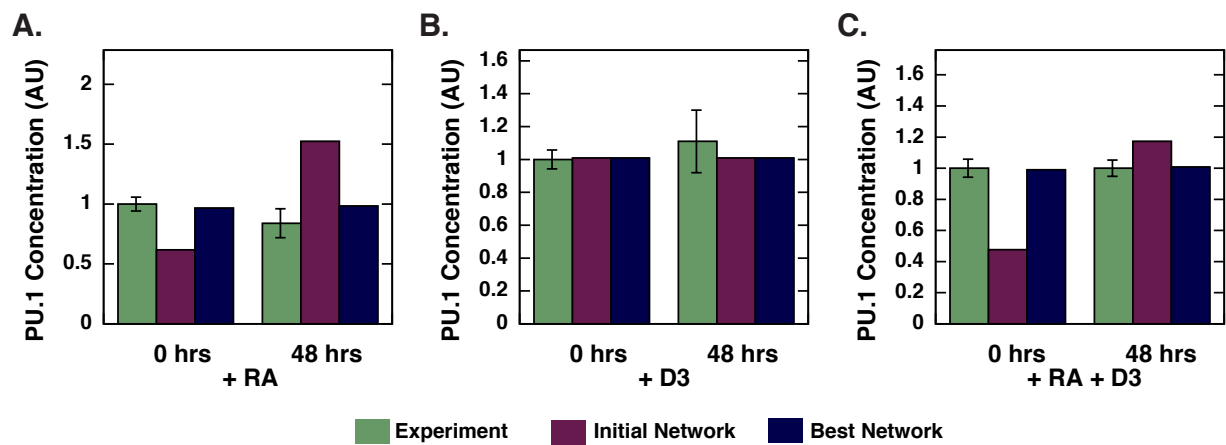


**Fig. 9:** Selected training results for the K562 cell line. A., B., C. Simulation and experimental results of change in PU.1 concentration due to RA, D3, and RA/D3 stimulus, respectively. Green denotes experimental data, pink denotes simulation data from the initial network, and blue denotes simulation data from the best network. The top parameter set is used, and error bars denote standard experimental error.

624 **Supplementary materials**

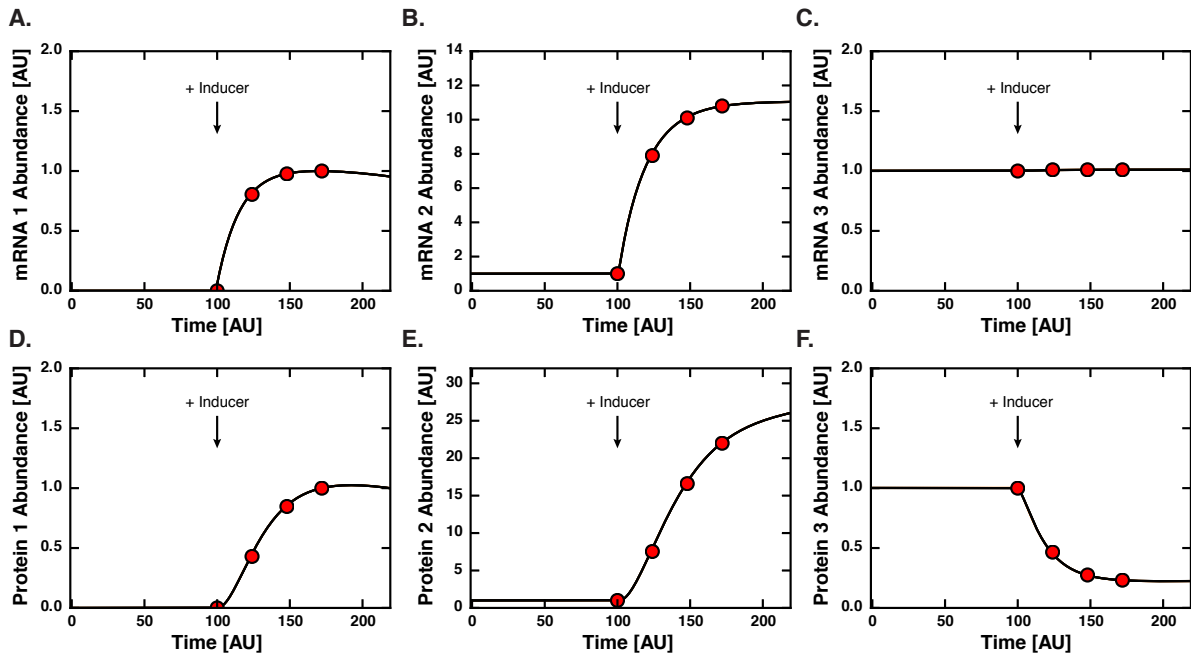


**Fig. S1:** Synthetic data running experiment 1 for true model of three node protein network. In experiment 1, inducer was added at Time = 100. A, B, C. Plots of mRNA concentration profiles for species 1, 2, and 3 after inducer added at Time = 100. D, E, F. Plots of protein concentration profiles for species 1, 2, and 3. Red dots denote data used for fitting (0, 24, 48, and 72 AU after stimulus).

625 **Table T1:** Training objective function list with objective number, species measured, experiment and trials used in

Objective #	Species	Experiment #	Trial
O1	$mRNA_1$	Exp1	1, 2
O2	$mRNA_2$	Exp1	1, 2
O3	$mRNA_3$	Exp1	1, 2
O4	$P_2$	Exp1	1, 2
O5	$P_3$	Exp1	1, 2
O6	$mRNA_1$	Exp2	2
O7	$mRNA_2$	Exp2	2
O8	$P_1$	Exp2	2
O9	$P_2$	Exp2	2
O10	$P_3$	Exp2	2
O11	$mRNA_1$	Exp3	2
O12	$mRNA_2$	Exp3	2
O13	$mRNA_3$	Exp3	2
O14	$P_1$	Exp3	2
O15	$P_3$	Exp3	2

627 **Table T2:** Prediction function list with prediction number, species measured, experiment and trials used in

Prediction #	Species	Experiment #	Trial
P1	$P_1$	Exp1	1, 2
P2	$mRNA_3$	Exp2	2
P3	$P_2$	Exp2	2

**Table T3:** Experiment list with stimulus, species for training, and species for validation

Experiment #	Stimulus	Training Species	Validation Species
1	At t = 100, Inducer = +10	$mRNA_1, mRNA_2,$ $mRNA_3, P_2, P_3$	$P_1$
2	At t = 100, Inducer = +10 and inhibit binding of protein 2	$mRNA_1, mRNA_2, P_1,$ $P_2, P_3$	$mRNA_3$
3	At t = 100, 124, 148, 172, 196, Inducer = +1	$mRNA_1, mRNA_2,$ $mRNA_3, P_1, P_3$	$P_2$

**Table T4:** Training objective function list with objective number, species measured, stimulus, and time points. The same 39 objective functions were used for all cell lines with data from [50].

Objective #	Species Measured	Stimulus	Time Point (hrs)
O1	C/EBP $\alpha$	1 $\mu$ M RA	48
O2	PU.1	1 $\mu$ M RA	48
O3	EGR1	1 $\mu$ M RA	48
O4	Gfi-1	1 $\mu$ M RA	48
O5	RAR $\alpha$	1 $\mu$ M RA	48
O6	VDR	1 $\mu$ M RA	48
O7	IRF-1	1 $\mu$ M RA	48
O8	Oct4	1 $\mu$ M RA	48
O9	AhR	1 $\mu$ M RA	48
O10	CD38	1 $\mu$ M RA	24, 48, 72
O11	CD11b	1 $\mu$ M RA	24, 48, 72
O12	CD14	1 $\mu$ M RA	24, 48, 72
O13	G1/G0	1 $\mu$ M RA	24, 48, 72
O14	C/EBP $\alpha$	0.5 $\mu$ M VD3	48
O15	PU.1	0.5 $\mu$ M VD3	48
O16	EGR1	0.5 $\mu$ M VD3	48
O17	Gfi-1	0.5 $\mu$ M VD3	48
O18	RAR $\alpha$	0.5 $\mu$ M VD3	48
O19	VDR	0.5 $\mu$ M VD3	48
O20	IRF-1	0.5 $\mu$ M VD3	48
O21	Oct4	0.5 $\mu$ M VD3	48
O22	AhR	0.5 $\mu$ M VD3	48
O23	CD38	0.5 $\mu$ M VD3	24, 48, 72
O24	CD11b	0.5 $\mu$ M VD3	24, 48, 72
O25	CD14	0.5 $\mu$ M VD3	24, 48, 72
O26	G1/G0	0.5 $\mu$ M VD3	24, 48, 72
O27	C/EBP $\alpha$	1 $\mu$ M RA, 0.5 $\mu$ M VD3	48
O28	PU.1	1 $\mu$ M RA, 0.5 $\mu$ M VD3	48
O29	EGR1	1 $\mu$ M RA, 0.5 $\mu$ M VD3	48
O30	Gfi-1	1 $\mu$ M RA, 0.5 $\mu$ M VD3	48
O31	RAR $\alpha$	1 $\mu$ M RA, 0.5 $\mu$ M VD3	48
O32	VDR	1 $\mu$ M RA, 0.5 $\mu$ M VD3	48

633

O33	IRF-1	1 $\mu$ M RA, 0.5 $\mu$ M VD3	48
O34	Oct4	1 $\mu$ M RA, 0.5 $\mu$ M VD3	48
O35	AhR	1 $\mu$ M RA, 0.5 $\mu$ M VD3	48
O36	CD38	1 $\mu$ M RA, 0.5 $\mu$ M VD3	24, 48, 72
O37	CD11b	1 $\mu$ M RA, 0.5 $\mu$ M VD3	24, 48, 72
O38	CD14	1 $\mu$ M RA, 0.5 $\mu$ M VD3	24, 48, 72
O39	G1/G0	1 $\mu$ M RA, 0.5 $\mu$ M VD3	24, 48, 72

## U937

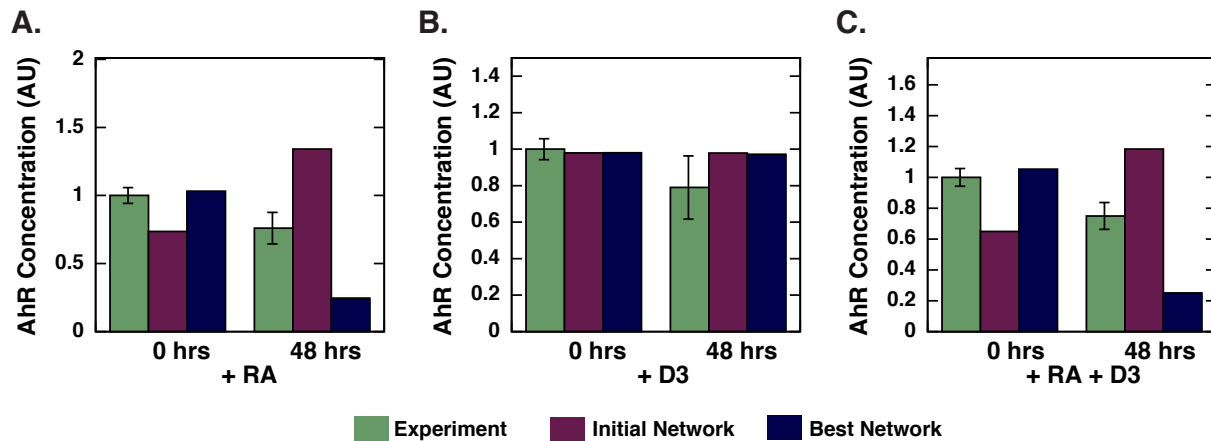


**Fig. S2:** Selected training results for the U937 cell line. A., B., C. Simulation and experimental results of change in AhR concentration due to RA, D3, and RA/D3 stimulus, respectively. Green denotes experimental data, pink denotes simulation data from the initial network, and blue denotes simulation data from the best network. The top parameter set is used, and error bars denote standard experimental error.

## HL60 R38+

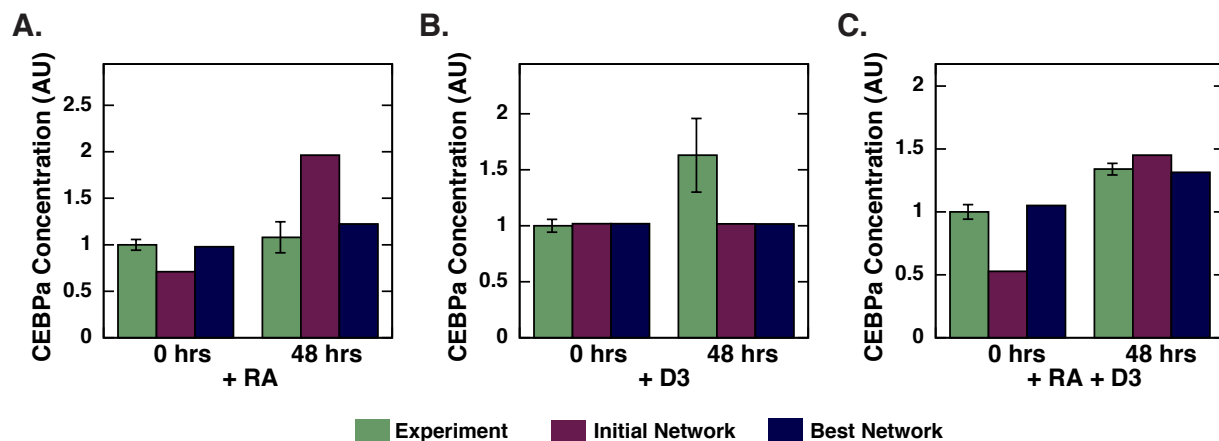


**Fig. S3:** Selected training results for the HL60 R38+ cell line. A., B., C. Simulation and experimental results of change in C/EBP $\alpha$  concentration due to RA, D3, and RA/D3 stimulus, respectively. Green denotes experimental data, pink denotes simulation data from the initial network, and blue denotes simulation data from the best network. The top parameter set is used, and error bars denote standard experimental error.

**Table T5:** Model Updates for K562 cell line with edge number, action, transcription factor, general effect, target gene, and new references

Edge Number	Action	Transcription Factor	General Effect	Target Gene	Reference(s)
6	deleted	RAR $\alpha$	upregulates	AhR	[9]
7	deleted	RAR $\alpha$	upregulates	C/EBP $\alpha$	
8	added	RAR $\alpha$	represses	Gfi-1	
9	deleted	RAR $\alpha$	upregulates	EGR1	
11	added	RAR $\alpha$	represses	AP-1	
14	added	RAR $\alpha$	represses	CD14	
20	added	VDR	represses	VDR	
22	added	VDR	upregulates	IRF-1	
23	added	VDR	represses	Oct1	
25	added	VDR	represses	C/EBP $\alpha$	
27	added	VDR	represses	EGR1	
31	added	VDR	represses	CD11b	
32	added	VDR	upregulates	CD14	[79]
34	added	VDR	upregulates	E2F	
38	added	PPAR $\gamma$	upregulates	VDR	
49	added	PPAR $\gamma$	represses	CD11b	
50	deleted	PPAR $\gamma$	upregulates	CD14	
52	deleted	PPAR $\gamma$	represses	E2F	
56	added	IRF-1	represses	VDR	
59	added	IRF-1	upregulates	Oct1	
61	added	IRF-1	upregulates	C/EBP $\alpha$	
63	added	IRF-1	upregulates	EGR1	
64	added	IRF-1	represses	PU.1	[91]
65	added	IRF-1	represses	AP-1	
67	added	IRF-1	upregulates	CD11b	
70	added	IRF-1	upregulates	E2F	
76	added	Oct1	represses	IRF-1	
77	added	Oct1	represses	Oct1	
78	added	Oct1	upregulates	AhR	
82	deleted	Oct1	upregulates	PU.1	
83	added	Oct1	upregulates	AP-1	
86	added	Oct1	upregulates	CD14	
87	added	Oct1	represses	p21	[66]
88	added	Oct1	upregulates	E2F	
89	added	Oct1	represses	p47phox	
90	added	Oct1	represses	Oct4	
92	added	AhR	upregulates	VDR	
97	added	AhR	represses	C/EBP $\alpha$	
99	added	AhR	upregulates	EGR1	
102	added	AhR	represses	CD38	
107	added	AhR	upregulates	p47phox	

636	110	added	C/EBP $\alpha$	represses	VDR	[44]
	117	added	C/EBP $\alpha$	represses	EGR1	
	118	deleted	C/EBP $\alpha$	upregulates	PU.1	
	121	added	C/EBP $\alpha$	upregulates	CD11b	
	122	switched	C/EBP $\alpha$	represses	CD14	
	128	added	Gfi-1	represses	VDR	
	129	added	Gfi-1	represses	PPAR $\gamma$	
	130	added	Gfi-1	represses	IRF-1	
	134	added	Gfi-1	represses	Gfi-1	
	141	deleted	Gfi-1	represses	p21	
	144	added	Gfi-1	represses	Oct4	
	146	added	EGR1	represses	VDR	
	147	switched	EGR1	represses	PPAR $\gamma$	
	150	added	EGR1	upregulates	AhR	
[56]	155	added	EGR1	upregulates	AP-1	[56]
	157	added	EGR1	upregulates	CD11b	
	162	added	EGR1	represses	Oct4	
	164	deleted	PU.1	upregulates	VDR	
	168	added	PU.1	represses	AhR	
	169	added	PU.1	represses	C/EBP $\alpha$	
	170	added	PU.1	upregulates	Gfi-1	
	173	deleted	PU.1	upregulates	AP-1	
	174	added	PU.1	represses	CD38	
	177	deleted	PU.1	upregulates	p21	
	178	added	PU.1	upregulates	E2F	
	179	switched	PU.1	represses	p47phox	
	180	added	PU.1	upregulates	Oct4	
	182	switched	AP-1	represses	VDR	
[56]	184	added	AP-1	upregulates	IRF-1	[56]
	187	deleted	AP-1	represses	C/EBP $\alpha$	
	188	added	AP-1	upregulates	Gfi-1	
	189	added	AP-1	upregulates	EGR1	
	195	switched	AP-1	represses	p21	
	198	added	AP-1	represses	Oct4	
	255	added	p21	represses	PPAR $\gamma$	
	257	added	p21	upregulates	Oct1	
	258	added	p21	represses	AhR	
	259	added	p21	represses	C/EBP $\alpha$	
	260	added	p21	represses	Gfi-1	
	263	added	p21	upregulates	AP-1	
	265	added	p21	represses	CD11b	
	274	added	E2F	upregulates	IRF-1	
	275	added	E2F	represses	Oct1	
	276	added	E2F	represses	AhR	

637	277	added	E2F	represses	C/EBP $\alpha$	[99]
	279	added	E2F	upregulates	EGR1	
	280	added	E2F	represses	PU.1	
	281	added	E2F	represses	AP-1	
	282	added	E2F	upregulates	CD38	
	283	added	E2F	represses	CD11b	
	284	added	E2F	represses	CD14	
	286	switched	E2F	represses	E2F	
	287	added	E2F	upregulates	p47phox	
	313	added	Oct4	upregulates	C/EBP $\alpha$	
	318	added	Oct4	represses	CD38	
	319	added	Oct4	upregulates	CD11b	
	320	added	Oct4	upregulates	CD14	
	322	added	Oct4	represses	E2F	
	324	added	Oct4	represses	Oct4	

**Table T6:** Model Updates for NB4 cell line with edge number, action, transcription factor, general effect, target gene, and new references

Edge Number	Action	Transcription Factor	General Effect	Target Gene	Reference(s)
3	added	RAR $\alpha$	represses	PPAR $\gamma$	
6	deleted	RAR $\alpha$	upregulates	AhR	
9	switched	RAR $\alpha$	represses	EGR1	
10	switched	RAR $\alpha$	represses	PU.1	
11	added	RAR $\alpha$	upregulates	AP-1	
13	added	RAR $\alpha$	upregulates	CD11b	
16	added	RAR $\alpha$	represses	E2F	
17	added	RAR $\alpha$	upregulates	p47phox	[5]
18	switched	RAR $\alpha$	upregulates	Oct4	[8]
22	added	VDR	represses	IRF-1	
24	added	VDR	upregulates	AhR	
26	added	VDR	upregulates	Gfi-1	
36	added	VDR	upregulates	Oct4	
38	added	PPAR $\gamma$	upregulates	VDR	
39	added	PPAR $\gamma$	represses	PPAR $\gamma$	
45	deleted	PPAR $\gamma$	represses	EGR1	
46	added	PPAR $\gamma$	represses	PU.1	
58	added	IRF-1	represses	IRF-1	
60	added	IRF-1	represses	AhR	
62	added	IRF-1	upregulates	Gfi-1	
63	added	IRF-1	upregulates	EGR1	
66	switched	IRF-1	represses	CD38	
70	added	IRF-1	represses	E2F	
72	added	IRF-1	upregulates	Oct4	
76	added	Oct1	upregulates	IRF-1	
77	added	Oct1	upregulates	Oct1	[74]
81	added	Oct1	represses	EGR1	
83	added	Oct1	upregulates	AP-1	[91]
86	added	Oct1	represses	CD14	
89	added	Oct1	upregulates	p47phox	
90	added	Oct1	represses	Oct4	
92	added	AhR	upregulates	VDR	
96	added	AhR	upregulates	AhR	
98	added	AhR	upregulates	Gfi-1	
100	switched	AhR	upregulates	PU.1	
103	added	AhR	upregulates	CD11b	
104	added	AhR	represses	CD14	
106	added	AhR	represses	E2F	[65]
110	added	C/EBP $\alpha$	upregulates	VDR	
111	switched	C/EBP $\alpha$	represses	PPAR $\gamma$	
113	added	C/EBP $\alpha$	upregulates	Oct1	

640	114	added	C/EBP $\alpha$	upregulates	AhR	[44]
	116	deleted	C/EBP $\alpha$	upregulates	Gfi-1	
	117	added	C/EBP $\alpha$	represses	EGR1	
	118	deleted	C/EBP $\alpha$	upregulates	PU.1	
	122	switched	C/EBP $\alpha$	represses	CD14	
	124	switched	C/EBP $\alpha$	upregulates	E2F	
	129	added	Gfi-1	represses	PPAR $\gamma$	
	133	deleted	Gfi-1	represses	C/EBP $\alpha$	
	138	added	Gfi-1	represses	CD38	
	143	added	Gfi-1	represses	p47phox	
	152	switched	EGR1	upregulates	Gfi-1	
	156	added	EGR1	represses	CD38	
	157	added	EGR1	upregulates	CD11b	
	167	added	PU.1	represses	Oct1	
	172	switched	PU.1	represses	PU.1	
	175	deleted	PU.1	upregulates	CD11b	[81]
	178	added	PU.1	upregulates	E2F	
	180	added	PU.1	represses	Oct4	
	182	deleted	AP-1	upregulates	VDR	
	186	added	AP-1	upregulates	AhR	
	188	added	AP-1	represses	Gfi-1	
	189	added	AP-1	upregulates	EGR1	
	190	deleted	AP-1	upregulates	PU.1	
	191	added	AP-1	represses	AP-1	
	193	added	AP-1	upregulates	CD11b	
	196	added	AP-1	upregulates	E2F	
	197	added	AP-1	represses	p47phox	
	254	added	p21	upregulates	VDR	
	255	added	p21	upregulates	PPAR $\gamma$	
	256	added	p21	represses	IRF-1	
	260	added	p21	upregulates	Gfi-1	
	262	added	p21	upregulates	PU.1	
	265	added	p21	upregulates	CD11b	
	268	added	p21	upregulates	E2F	
	272	added	E2F	upregulates	VDR	
	273	added	E2F	represses	PPAR $\gamma$	
	274	added	E2F	upregulates	IRF-1	
	276	added	E2F	upregulates	AhR	
	281	added	E2F	upregulates	AP-1	
	283	added	E2F	upregulates	CD11b	
	284	added	E2F	upregulates	CD14	
	286	switched	E2F	represses	E2F	
	288	added	E2F	represses	Oct4	
	309	added	Oct4	upregulates	PPAR $\gamma$	

641

310	added	Oct4	represses	IRF-1	
312	added	Oct4	upregulates	AhR	
314	added	Oct4	upregulates	Gfi-1	
317	added	Oct4	represses	AP-1	
320	added	Oct4	upregulates	CD14	

**Table T7:** Model Updates for WT-HL60 cell line with edge number, action, transcription factor, general effect, target gene, and new references

Edge Number	Action	Transcription Factor	General Effect	Target Gene	Reference(s)
2	added	RAR $\alpha$	represses	VDR	[5]
3	added	RAR $\alpha$	upregulates	PPAR $\gamma$	
5	added	RAR $\alpha$	represses	Oct1	
6	switched	RAR $\alpha$	represses	AhR	
7	switched	RAR $\alpha$	represses	C/EBP $\alpha$	
8	added	RAR $\alpha$	represses	Gfi-1	
13	added	RAR $\alpha$	upregulates	CD11b	
14	added	RAR $\alpha$	represses	CD14	
17	added	RAR $\alpha$	upregulates	p47phox	
21	deleted	VDR	upregulates	PPAR $\gamma$	
27	added	VDR	represses	EGR1	
34	added	VDR	represses	E2F	
38	added	PPAR $\gamma$	upregulates	VDR	
39	added	PPAR $\gamma$	represses	PPAR $\gamma$	
40	switched	PPAR $\gamma$	represses	IRF-1	
42	added	PPAR $\gamma$	upregulates	AhR	
45	switched	PPAR $\gamma$	upregulates	EGR1	
48	deleted	PPAR $\gamma$	upregulates	CD38	
49	added	PPAR $\gamma$	upregulates	CD11b	
50	switched	PPAR $\gamma$	represses	CD14	
53	deleted	PPAR $\gamma$	represses	p47phox	
56	added	IRF-1	upregulates	VDR	
66	switched	IRF-1	represses	CD38	
68	added	IRF-1	represses	CD14	
70	added	IRF-1	represses	E2F	
74	switched	Oct1	represses	VDR	
78	added	Oct1	upregulates	AhR	
79	added	Oct1	upregulates	C/EBP $\alpha$	[91]
83	added	Oct1	upregulates	AP1	
85	added	Oct1	upregulates	CD11b	
87	added	Oct1	upregulates	p21	
88	added	Oct1	represses	E2F	
89	added	Oct1	represses	p47phox	
95	added	AhR	upregulates	Oct1	
96	added	AhR	represses	AhR	
100	switched	AhR	upregulates	PU.1	
101	deleted	AhR	upregulates	AP1	
103	added	AhR	represses	CD11b	[65]
104	added	AhR	upregulates	CD14	
106	added	AhR	upregulates	E2F	[65]
110	added	C/EBP $\alpha$	upregulates	VDR	

644	113	added	C/EBP $\alpha$	represses	Oct1	[95]
	118	switched	C/EBP $\alpha$	represses	PU.1	
	119	added	C/EBP $\alpha$	upregulates	AP1	
	122	deleted	C/EBP $\alpha$	upregulates	CD14	
	123	deleted	C/EBP $\alpha$	upregulates	p21	
	125	added	C/EBP $\alpha$	upregulates	p47phox	
	126	added	C/EBP $\alpha$	represses	Oct4	
	136	deleted	Gfi-1	represses	PU.1	
	141	deleted	Gfi-1	represses	p21	
	142	deleted	Gfi-1	represses	E2F	
	143	added	Gfi-1	represses	p47phox	
	148	added	EGR1	upregulates	IRF-1	
	149	added	EGR1	represses	Oct1	
	151	added	EGR1	represses	C/EBP $\alpha$	
	155	added	EGR1	represses	AP1	
	158	deleted	EGR1	upregulates	CD14	
	159	added	EGR1	upregulates	p21	
	164	deleted	PU.1	upregulates	VDR	
	165	deleted	PU.1	represses	PPAR $\gamma$	
	167	added	PU.1	represses	Oct1	
	174	added	PU.1	upregulates	CD38	
	176	added	PU.1	represses	CD14	
	179	deleted	PU.1	upregulates	p47phox	
	181	added	AP1	upregulates	RAR $\alpha$	
	182	deleted	AP1	upregulates	VDR	
	183	added	AP1	represses	PPAR $\gamma$	
	185	added	AP1	represses	Oct1	
	191	added	AP1	represses	AP1	
	193	added	AP1	upregulates	CD11b	
	254	added	p21	upregulates	VDR	
	257	added	p21	upregulates	Oct1	
	258	added	p21	upregulates	AhR	
	261	added	p21	represses	EGR1	
	262	added	p21	upregulates	PU.1	
	264	added	p21	upregulates	CD38	
	270	added	p21	upregulates	Oct4	
	272	added	E2F	represses	VDR	
	273	added	E2F	represses	PPAR $\gamma$	
	274	added	E2F	upregulates	IRF-1	
	275	added	E2F	represses	Oct1	
	276	added	E2F	upregulates	AhR	
	281	added	E2F	represses	AP1	
	283	added	E2F	represses	CD11b	
	312	added	Oct4	represses	AhR	

645

314	added	Oct4	upregulates	Gfi-1	
316	added	Oct4	upregulates	PU.1	
317	added	Oct4	represses	AP1	
319	added	Oct4	represses	CD11b	
320	added	Oct4	represses	CD14	
323	added	Oct4	upregulates	p47phox	

**Table T8:** Model Updates for HL60 R38+ cell line with edge number, action, transcription factor, general effect, target gene, and new references

Edge Number	Action	Transcription Factor	General Effect	Target Gene	Reference(s)
10	deleted	RAR $\alpha$	upregulates	PU.1	
13	added	RAR $\alpha$	upregulates	CD11b	
16	added	RAR $\alpha$	upregulates	E2F	
18	deleted	RAR $\alpha$	upregulates	Oct4	
21	switched	VDR	upregulates	PPAR $\gamma$	
22	added	VDR	upregulates	IRF-1	
23	added	VDR	upregulates	Oct1	
29	added	VDR	upregulates	AP1	[97]
31	added	VDR	upregulates	CD11b	
32	added	VDR	upregulates	CD14	[79]
36	added	VDR	upregulates	Oct4	
40	deleted	PPAR $\gamma$	upregulates	IRF-1	
44	added	PPAR $\gamma$	upregulates	Gfi-1	
52	deleted	PPAR $\gamma$	upregulates	E2F	
54	added	PPAR $\gamma$	upregulates	Oct4	
59	added	IRF-1	upregulates	Oct1	
62	added	IRF-1	upregulates	Gfi-1	
63	added	IRF-1	upregulates	EGR1	
64	added	IRF-1	upregulates	PU.1	
69	deleted	IRF-1	upregulates	p21	
71	added	IRF-1	upregulates	p47phox	
76	added	Oct1	upregulates	IRF-1	
81	added	Oct1	upregulates	EGR1	
82	switched	Oct1	upregulates	PU.1	
88	added	Oct1	upregulates	E2F	
90	added	Oct1	upregulates	Oct4	
94	deleted	AhR	upregulates	IRF-1	
99	added	AhR	upregulates	EGR1	[66]
100	deleted	AhR	upregulates	PU.1	
102	added	AhR	upregulates	CD38	
105	added	AhR	upregulates	p21	
107	added	AhR	upregulates	p47phox	
111	deleted	C/EBP $\alpha$	upregulates	PPAR $\gamma$	
112	added	C/EBP $\alpha$	upregulates	IRF-1	
114	added	C/EBP $\alpha$	upregulates	AhR	
116	switched	C/EBP $\alpha$	upregulates	Gfi-1	
117	added	C/EBP $\alpha$	upregulates	EGR1	
118	switched	C/EBP $\alpha$	upregulates	PU.1	
119	added	C/EBP $\alpha$	upregulates	AP1	
120	added	C/EBP $\alpha$	upregulates	CD38	
125	added	C/EBP $\alpha$	upregulates	p47phox	

648	131	added	Gfi-1	upregulates	Oct1	
	132	added	Gfi-1	upregulates	AhR	
	133	deleted	Gfi-1	upregulates	C/EBP $\alpha$	
	135	deleted	Gfi-1	upregulates	EGR1	
	139	added	Gfi-1	upregulates	CD11b	
	142	deleted	Gfi-1	upregulates	E2F	
	150	added	EGR1	upregulates	AhR	
	152	deleted	EGR1	upregulates	Gfi-1	
	154	added	EGR1	upregulates	PU.1	[37]
	156	added	EGR1	upregulates	CD38	
	161	added	EGR1	upregulates	p47phox	
	165	switched	PU.1	upregulates	PPAR $\gamma$	
	167	added	PU.1	upregulates	Oct1	
	170	added	PU.1	upregulates	Gfi-1	
	173	switched	PU.1	upregulates	AP1	
	175	deleted	PU.1	upregulates	CD11b	
	179	deleted	PU.1	upregulates	p47phox	
	183	added	AP1	upregulates	PPAR $\gamma$	[95]
	188	added	AP1	upregulates	Gfi-1	
	192	added	AP1	upregulates	CD38	
	195	deleted	AP1	upregulates	p21	
	256	added	p21	upregulates	IRF-1	
	261	added	p21	upregulates	EGR1	
	266	added	p21	upregulates	CD14	
	269	added	p21	upregulates	p47phox	
	270	added	p21	upregulates	Oct4	
	274	added	E2F	upregulates	IRF-1	
	279	added	E2F	upregulates	EGR1	
	310	added	Oct4	upregulates	IRF-1	
	312	added	Oct4	upregulates	AhR	
	315	added	Oct4	upregulates	EGR1	
	318	added	Oct4	upregulates	CD38	
	320	added	Oct4	upregulates	CD14	

**Table T9:** Model Updates for HL60 R38- cell line with edge number, action, transcription factor, general effect, target gene, and new references

Edge Number	Action	Transcription Factor	General Effect	Target Gene	Reference(s)
7	deleted	RAR $\alpha$	upregulates	C/EBP $\alpha$	
9	switched	RAR $\alpha$	represses	EGR1	
14	added	RAR $\alpha$	represses	CD14	
16	added	RAR $\alpha$	upregulates	E2F	
21	deleted	VDR	upregulates	PPAR $\gamma$	
25	added	VDR	represses	C/EBP $\alpha$	
26	added	VDR	represses	Gfi-1	
29	added	VDR	represses	AP-1	[97]
40	deleted	PPAR $\gamma$	upregulates	IRF-1	
41	switched	PPAR $\gamma$	represses	Oct1	
43	switched	PPAR $\gamma$	represses	C/EBP $\alpha$	
46	added	PPAR $\gamma$	upregulates	PU.1	
47	switched	PPAR $\gamma$	upregulates	AP-1	
49	added	PPAR $\gamma$	upregulates	CD11b	
57	added	IRF-1	upregulates	PPAR $\gamma$	
58	added	IRF-1	upregulates	IRF-1	
62	added	IRF-1	represses	Gfi-1	
63	added	IRF-1	represses	EGR1	
64	added	IRF-1	upregulates	PU.1	
65	added	IRF-1	represses	AP-1	
66	deleted	IRF-1	upregulates	CD38	
67	added	IRF-1	upregulates	CD11b	
70	added	IRF-1	upregulates	E2F	
71	added	IRF-1	represses	p47phox	
73	added	Oct1	represses	RAR $\alpha$	[53]
75	added	Oct1	upregulates	PPAR $\gamma$	
78	added	Oct1	represses	AhR	
83	added	Oct1	represses	AP-1	[91]
87	added	Oct1	upregulates	p21	
89	added	Oct1	represses	p47phox	
91	added	AhR	upregulates	RAR $\alpha$	[96]
93	added	AhR	upregulates	PPAR $\gamma$	
94	deleted	AhR	upregulates	IRF-1	
100	deleted	AhR	represses	PU.1	
101	switched	AhR	represses	AP-1	
104	added	AhR	represses	CD14	
105	added	AhR	represses	p21	
109	added	C/EBP $\alpha$	upregulates	RAR $\alpha$	
110	added	C/EBP $\alpha$	upregulates	VDR	
111	deleted	C/EBP $\alpha$	upregulates	PPAR $\gamma$	
114	added	C/EBP $\alpha$	upregulates	AhR	

651	116	deleted	C/EBP $\alpha$	upregulates	Gfi-1	
	118	deleted	C/EBP $\alpha$	upregulates	PU.1	
	119	added	C/EBP $\alpha$	upregulates	AP-1	
	124	deleted	C/EBP $\alpha$	represses	E2F	
	125	added	C/EBP $\alpha$	upregulates	p47phox	
	132	added	Gfi-1	represses	AhR	
	133	deleted	Gfi-1	represses	C/EBP $\alpha$	
	139	added	Gfi-1	represses	CD11b	
	140	added	Gfi-1	represses	CD14	
	141	deleted	Gfi-1	represses	p21	
	146	added	EGR1	represses	VDR	
	150	added	EGR1	upregulates	AhR	
	156	added	EGR1	upregulates	CD38	
	158	deleted	EGR1	upregulates	CD14	
	160	added	EGR1	represses	E2F	
	162	added	EGR1	upregulates	Oct4	
	176	added	PU.1	upregulates	CD14	
	178	added	PU.1	represses	E2F	
	180	added	PU.1	upregulates	Oct4	
	194	added	AP-1	represses	CD14	
	195	switched	AP-1	represses	p21	
	256	added	p21	upregulates	IRF-1	
	263	added	p21	upregulates	AP-1	
	266	added	p21	represses	CD14	
	269	added	p21	represses	p47phox	
	272	added	E2F	represses	VDR	
	275	added	E2F	represses	Oct1	
	279	added	E2F	represses	EGR1	
	283	added	E2F	upregulates	CD11b	
	309	added	Oct4	upregulates	PPAR $\gamma$	
	317	added	Oct4	represses	AP-1	
	318	added	Oct4	upregulates	CD38	
	319	added	Oct4	upregulates	CD11b	
	321	added	Oct4	upregulates	p21	
	323	added	Oct4	upregulates	p47phox	

**Table T10:** Model Updates for U937 cell line with edge number, action, transcription factor, general effect, target gene, and new references

Edge Number	Action	Transcription Factor	General Effect	Target Gene	Reference(s)
2	added	RAR $\alpha$	upregulates	VDR	[53]
13	added	RAR $\alpha$	upregulates	CD11b	
14	added	RAR $\alpha$	represses	CD14	
17	added	RAR $\alpha$	upregulates	p47phox	
27	added	VDR	upregulates	EGR1	
36	added	VDR	upregulates	Oct4	
44	added	PPAR $\gamma$	upregulates	Gfi-1	
48	deleted	PPAR $\gamma$	upregulates	CD38	
62	added	IRF-1	upregulates	Gfi-1	
71	added	IRF-1	represses	p47phox	
72	added	IRF-1	represses	Oct4	
73	added	Oct1	upregulates	RAR $\alpha$	
75	added	Oct1	represses	PPAR $\gamma$	
77	added	Oct1	upregulates	Oct1	
80	added	Oct1	represses	Gfi-1	
92	added	AhR	upregulates	VDR	
96	added	AhR	upregulates	AhR	
97	added	AhR	upregulates	C/EBP $\alpha$	
100	switched	AhR	upregulates	PU.1	[44]
103	added	AhR	upregulates	CD11b	
106	added	AhR	represses	E2F	
110	added	C/EBP $\alpha$	upregulates	VDR	
114	added	C/EBP $\alpha$	upregulates	AhR	
117	added	C/EBP $\alpha$	represses	EGR1	
119	added	C/EBP $\alpha$	represses	AP-1	
129	added	Gfi-1	represses	PPAR $\gamma$	
137	added	Gfi-1	represses	AP-1	
139	added	Gfi-1	represses	CD11b	
153	added	EGR1	upregulates	EGR1	[56]
170	added	PU.1	represses	Gfi-1	
178	added	PU.1	represses	E2F	
180	added	PU.1	upregulates	Oct4	
188	added	AP-1	upregulates	Gfi-1	
194	added	AP-1	upregulates	CD14	
196	added	AP-1	upregulates	E2F	
198	added	AP-1	upregulates	Oct4	
254	added	p21	represses	VDR	
268	added	p21	represses	E2F	
312	added	Oct4	represses	AhR	
317	added	Oct4	represses	AP-1	
320	added	Oct4	represses	CD14	

